



A Family of Non-Monotonic Toral Mixing Maps

J. Myers Hill¹ · R. Sturman² · M. C. T. Wilson³

Received: 16 December 2021 / Accepted: 28 February 2022 / Published online: 1 April 2022
© The Author(s) 2022

Abstract

We establish the mixing property for a family of Lebesgue measure preserving toral maps composed of two piecewise linear shears, the first of which is non-monotonic. The maps serve as a basic model for the ‘stretching and folding’ action in laminar fluid mixing, in particular flows where boundary conditions give rise to non-monotonic flow profiles. The family can be viewed as the parameter space between two well-known systems, Arnold’s Cat Map and a map due to Cerbelli and Giona, both of which possess finite Markov partitions and straightforward to prove mixing properties. However, no such finite Markov partitions appear to exist for the present family, so establishing mixing properties requires a different approach. In particular, we follow a scheme of Katok and Strelcyn, proving strong mixing properties with respect to the Lebesgue measure on two open parameter spaces. Finally, we comment on the challenges in extending these mixing windows and the potential for using the same approach to prove mixing properties in similar systems.

Keywords Low-dimensional dynamics · Non-uniform hyperbolicity · Mixing · Deterministic chaos

Mathematics Subject Classification 37A25

1 Introduction

Two-dimensional measure-preserving discrete-time dynamical systems are both rich in behaviour and relevant to a wide variety of applications. For example, as stroboscopic maps of fluid flow they constitute a model of kinematic mixing (Ottino 1989); as

Communicated by George Haller.

✉ J. Myers Hill
scjmh@leeds.ac.uk

¹ EPSRC CDT in Fluid Dynamics, University of Leeds, Leeds LS2 9JT, UK

² School of Mathematics, University of Leeds, Leeds LS2 9JT, UK

³ School of Mechanical Engineering, University of Leeds, Leeds LS2 9JT, UK

canonical examples of Hamiltonian systems such as forced pendulums or kicked rotators (Ott 2002); as fundamental models in fast dynamo theory (Childress and Gilbert 1995) and quantum chaos (Keating 1991). The richness of the dynamical behaviour can be seen in the observations that the dynamics may be integrable, but also may exhibit chaotic behaviour. That is, within two-dimensional maps, hyperbolicity is compatible with area-preservation, allowing access to the complete ergodic hierarchy, including ergodicity, measure-theoretic mixing, the Bernoulli property, etc.

This richness can be illustrated by considering the family of maps given by the transformation $H : (x, y) \rightarrow (x', y')$ of the 2-torus \mathbb{T}^2 into itself, given by

$$x' = x + f(y) \quad (1)$$

$$y' = y + x'. \quad (2)$$

Interpreting H as the composition of a pair of shears $H = G \circ F$, with $F(x, y) = x + f(y)$, $G(x, y) = y + x$ clarifies that Lebesgue measure is preserved by H , regardless of the choice of f . In the case of the Cat Map, $f(y) = y$ imposes a constant, hyperbolic, Jacobian at every point in \mathbb{T}^2 . This fact provides the means to establish immediately dynamical properties, such as unstable manifolds all lying in the same direction, a positive Lyapunov exponent for every trajectory, and ergodic properties, such as strong mixing, the Bernoulli property and exponential decay of correlations. The uniform hyperbolicity of the Cat Map might be a desirable property, but is also strong enough to preclude many applications.

The strict condition of uniformity of the hyperbolicity may be broken in a number of ways. A typical method is to slow down the expansion of tangent vectors. The first such example of a non-uniformly hyperbolic C^∞ area-preserving map on \mathbb{T}^2 was the Katok map (Katok 1979), in which trajectories near the hyperbolic fixed point at the origin are slowed down, with that fixed point becoming neutral. This is sufficient to produce zero Lyapunov exponents for some trajectories (although at almost every initial condition these remain nonzero), and thus non-hyperbolicity. In spite of the loss of uniform hyperbolicity, exponential decay of correlations are retained (Pesin et al. 2019).

Another example which breaks the uniformity of expansion is a linked twist map. Defined on a subset of \mathbb{T}^2 we replace function $f(y)$ with a piecewise smooth, non-decreasing function $\hat{f}(y)$, such that $d\hat{f}/dy = 0$ over some sub-interval of $[0, 1]$. Now unstable leaves are oriented in a continuum of directions, but, crucially, all contained in the positive quadrant of tangent space, which makes the demonstration of the mixing property relatively straightforward. Such a map retains the Bernoulli property of the Cat Map (Przytycki 1983), but the rate of mixing is slowed to polynomial decay of correlations (Sturman and Springham 2013; Springham and Sturman 2014).

One more example destroying the simplicity of the Cat Map can be found in the discontinuous sawtooth map. Here, $f(y) = Cy$, with $C > 0$, so that $C = 1$ recovers the Cat Map. When K is any other positive integer, the map is continuous on the torus and the same analysis applied. When K is non-integer however, the map becomes discontinuous, and although stable and unstable manifolds exist locally almost everywhere, these may be arbitrarily short, cut up by the dense countable set of discontinuity lines

created by iterating the map. Nevertheless, the map retains its ergodicity (Vaianti 1992) as the parameter C is perturbed from an integer. A further example destroying the simplicity of the Cat Map is found in Liverani (2004), taking $f(y) = y - \frac{1+\varepsilon}{2\pi} \sin(2\pi y)$ with $\varepsilon \geq -1$. At $\varepsilon = -1$ we recover the Cat Map and any perturbation $\varepsilon > -1$ gives a shear that is nonlinear and smooth. The mixing property is preserved under small perturbations, but critically only when f is non-decreasing ($\varepsilon \leq 0$).

For all the above examples, the map could be described as monotonic, in the sense that $f(y)$ is non-decreasing in each case. Much more complicated dynamics is possible if this condition is broken, as can be seen in the rich behaviour of the Chirikov–Taylor Standard Map (Chirikov 1971). This well-known map, for which $f(y) = \frac{K}{2\pi} \sin 2\pi y$, where K is a parameter, can exhibit co-existence of invariant circles, elliptic islands and chaotic seas, due to the lack of an invariant cone in tangent space. The wider range of possible directions for unstable leaves allows for the possibility of expansion being immediately counteracted in the following iterate, and the consequent failure of hyperbolicity.

A piecewise–linear version of the standard map was studied in Wojtkowski (1981) and Bullett (1986), where $f(y) = K(|y - 1/2| - 1/4)$, and shown for certain parameter values to be non-uniformly hyperbolic ($K \geq 4$) and mixing ($K > K_0 \approx 4.0329$). For $K < 4$, the map admits both chaotic and elliptic invariant domains; mixing properties over such a chaotic domain are shown for the $K = 1$ map in Liverani and Wojtkowski (1995). A different piecewise–linear adaptation of the standard map is that introduced by Cerbelli and Giona (2005), and proposed as a ‘continuous archetype of area-preserving non-uniform chaos’. This map takes $f(y) = 2y$ if $y \in [0, 1/2]$ and $f(y) = 2(1 - y)$ if $y \in [1/2, 1]$. Like the Cat Map, the Cerbelli–Giona map (hereafter CG map) has a finite Markov partition (MacKay 2006), and so only a finite number of possible directions for piecewise linear segments in the unstable and stable leaves.

Various generalisations to the CG map have been proposed, for example, in Demers and Wojtkowski (2009) a family of maps designed to preserve the Markov structure is examined, while in MacKay (2006) a number of perturbations preserving the pseudo-Anosov nature of the map are proposed. A smooth perturbation was considered in Cerbelli and Giona (2008) and dynamical properties such as topological entropy were studied numerically, but the mixing property was not demonstrated. Here, we take $f(y) = y/(1 - \eta)$ if $y \in [0, 1 - \eta]$ and $f(y) = (1 - y)/\eta$ if $y \in [1 - \eta, 1]$ with $0 < \eta < 1/2$. Note that as $\eta \rightarrow 1/2$ we recover the CG map, and as $\eta \rightarrow 0$ we limit pointwise onto the Cat Map.

We focus on the parameter space between the Cat map and the CG map, demonstrating the Bernoulli property over two subsets of $0 < \eta < 1/2$. In Sect. 2, we state our results and these subsets explicitly, while in Sect. 3 we summarise the steps the proof requires. Section 4 deals with the parameter range near the Cat Map, and Sect. 5 with parameters near the CG Map. To keep the argument concise, we move three derivations from Sect. 5 to Appendix, Sect. 7. We conclude with some final remarks in Sect. 6. Explicit expressions for certain coordinates used in Sects. 4 and 5 are given as supplementary material.

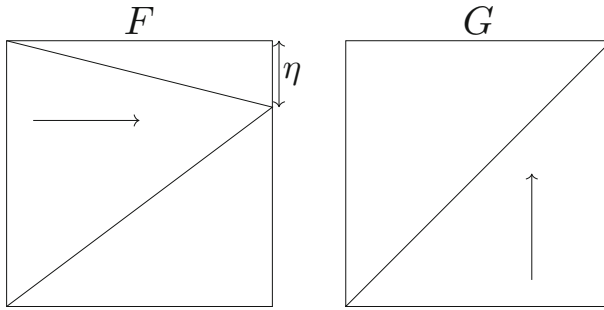


Fig. 1 A family of area preserving maps $H = G \circ F$ parameterised by $0 < \eta < 1/2$. The pointwise limit $\eta \rightarrow 0$ gives the Cat Map and taking $\eta \rightarrow 1/2$ gives Cerbelli and Giona’s map, both with well-understood mixing properties

2 Statement of Results

We consider the Lebesgue measure preserving map $H : \mathbb{T}^2 \rightarrow \mathbb{T}^2$, taken as the composition of two orthogonal shears $H = G \circ F$, shown in Fig. 1. Taking local coordinates $(x, y) \in (\mathbb{R}/\mathbb{Z})^2$, F maps

$$(x, y) \mapsto \begin{cases} \left(x + \frac{1}{1-\eta}y, y\right) \bmod 1 & \text{for } y \leq 1 - \eta \\ \left(x + \frac{1}{\eta}(1 - y), y\right) \bmod 1 & \text{for } y \geq 1 - \eta \end{cases}$$

and G maps $(x, y) \mapsto (x, y + x) \bmod 1$, where η is some real parameter $0 \leq \eta \leq \frac{1}{2}$. Note that H is piecewise linear, with derivative

$$DH_1 = \begin{pmatrix} 1 & \frac{1}{1-\eta} \\ 1 & \frac{2-\eta}{1-\eta} \end{pmatrix}$$

for $0 < y < 1 - \eta$, and

$$DH_0 = \begin{pmatrix} 1 & -\frac{1}{\eta} \\ 1 & \frac{\eta-1}{\eta} \end{pmatrix}$$

for $1 - \eta < y < 1$. DH , then, is defined everywhere but the set $\mathcal{D} = \{(x, y) \mid y \in \{0, 1 - \eta\}\}$. The inverse map $H^{-1} = F^{-1} \circ G^{-1}$ is differentiable outside of the set $\mathcal{D}' = G(\mathcal{D})$.

The aim of this paper is to prove mixing properties for H over a wide parameter range. In particular, we prove:

Theorem 1 *H has the Bernoulli property for $0 < \eta < \eta_1$ and $\eta_2 \leq \eta < \eta_3$ where $\eta_1 \approx 0.324$, $\eta_2 \approx 0.415$, and $\eta_3 \approx 0.491$.*

3 Proof Outline

Our scheme for proving the Bernoulli property is to satisfy the qualifications given in the following theorem from Katok and Strelcyn (1986), paraphrased in Sturman et al. (2006).

Theorem 2 (Katok and Strelcyn) *Let $f : X \rightarrow X$ be a measure preserving map on a measure space (X, \mathcal{F}, μ) such that f is C^2 smooth outside of a singularity set S where differentiability fails. Suppose that the Katok–Strelcyn conditions hold:*

- (KS1): $\exists a, C_1 > 0$ s.t. $\forall \epsilon > 0, \mu(B_\epsilon(S)) \leq C_1 \epsilon^a$.
- (KS2): $\exists b, C_2 > 0$ s.t. $\forall z \in X \setminus S, \|D_z^2 f\| \leq C_2 d(z, S)^{-b}$ where $D_z^2 f$ is the second derivative of f at z .
- (KS3): Lyapunov exponents exist and are nonzero almost everywhere.

Then at almost every z we can define local unstable and stable manifolds $\gamma_u(z)$ and $\gamma_s(z)$. Suppose that the manifold intersection property holds:

- (M): For almost any $z, z' \in X, \exists m, n$ s.t. $f^m(\gamma_u(z)) \cap f^{-n}(\gamma_s(z')) \neq \emptyset$.

Then, f is ergodic. Furthermore, the Bernoulli property holds, provided we can show the repeated manifold intersection property:

- (MR): For almost any $z, z' \in X$ we can find M, N such that for all $m > M$ and $n > N, f^m(\gamma_u(z)) \cap f^{-n}(\gamma_s(z')) \neq \emptyset$.

The scheme extends Pesin theory (establishing ergodic properties of C^2 smooth non-uniformly hyperbolic systems, Pesin 1977) to systems which are smooth outside of some singularity set. The conditions (KS1-2) ensure that this set has manageable influence and follow easily from our map’s definition. We take our map as $f = H$, our domain as $X = \mathbb{T}^2$, and our singularity set as $S = \mathcal{D}$. Taking μ to be the Lebesgue measure on \mathbb{T}^2 , clearly $\mu(S) = 0$. When we say ‘for almost any $z \in \mathbb{T}^2$ ’, we will be referring to the full measure set $X' = \mathbb{T}^2 \setminus S_\infty, S_\infty = \bigcup_{k \geq 0} H^{-k}(\mathcal{D}) \cup \bigcup_{k \geq 0} H^k(\mathcal{D})$, where H and all its powers $H^k, k \in \mathbb{Z}$ are differentiable. Since we can cover \mathcal{D} with arbitrarily thin rectangles, (KS1) follows for some $C_1 > 0$ with $a = 1$. Since H is piecewise linear, (KS2) follows trivially.

Moving onto (KS3), we define the (forwards-time) Lyapunov exponent at a point $z \in \mathbb{T}^2$ in direction $v \in \mathbb{R}^2$ by

$$\chi(z, v) = \lim_{n \rightarrow \infty} \frac{1}{n} \log \|DH_z^n v\|,$$

where

$$DH_z^n = DH_{H^{n-1}(z)} \cdots \cdots DH_{H(z)} \cdot DH_z$$

is well defined at almost every z . We define $\log^+(\cdot) = \max\{\log(\cdot), 0\}$ and let $\|\cdot\|_{\text{op}}$ be the operator norm. Existence of Lyapunov exponents almost everywhere follows from Oseledets’ theorem (Oseledets 1968) provided that $\log^+ \|DH\|_{\text{op}}$ is integrable. This clearly holds, so our first substantial task is proving that these exponents are

nonzero. A particular form of Oseledets’ theorem in two dimensions is useful here. We paraphrase from Viana (2014):

Theorem 3 (Oseledets, Viana) *Let $F : X \times \mathbb{R}^2 \rightarrow X \times \mathbb{R}^2$ be given by $F(x, v) = (f(x), A(x)v)$ for some measure preserving map f on a 2-dimensional manifold X and some measurable function $A : X \rightarrow \text{GL}(2)$. Suppose $\log^+ \|A^{\pm 1}\|$ are integrable and define*

$$\lambda_+(x) = \lim_{n \rightarrow \infty} \frac{1}{n} \log \|A^n(x)\|, \quad \lambda_-(x) = \lim_{n \rightarrow \infty} \frac{1}{n} \log \|(A^n(x))^{-1}\|^{-1},$$

where $A^n(x) = A(f^{n-1}(x)) \cdots A(f(x)) \cdot A(x)$. Then, for almost every $x \in X$,

1. either $\lambda_-(x) = \lambda_+(x)$ and

$$\lim_{n \rightarrow \infty} \frac{1}{n} \log \|A^n(x)v\| = \lambda_{\pm}(x) \quad \forall v \in \mathbb{R}^2 \setminus \{0\}$$

2. or $\lambda_+(x) > \lambda_-(x)$ and there exists a vector line $E_x^s \subset \mathbb{R}^2$ such that

$$\lim_{n \rightarrow \infty} \frac{1}{n} \log \|A^n(x)v\| = \begin{cases} \lambda_-(x) & \text{for } v \in E_x^s \setminus \{0\}, \\ \lambda_+(x) & \text{for } v \in \mathbb{R}^2 \setminus E_x^s. \end{cases}$$

Corollary 1 *Further assuming that A takes values in $\text{SL}(2)$ gives $\lambda_-(x) = -\lambda_+(x)$. Hence, if at some x , there exists $v_0 \in \mathbb{R}^2$ with $\lim_n \frac{1}{n} \log \|A^n(x)v_0\| \neq 0$, it follows that $\lim_n \frac{1}{n} \log \|A^n(x)v\| \neq 0$ for all nonzero vectors v .*

Applying this corollary to the cocycle generated by the derivative DH of our map H gives an efficient scheme for establishing nonzero Lyapunov exponents. We let $A^n(z) = DH_z^n$, which takes values in $\text{SL}(2)$. If there exists v_0 such that $\|DH_z^n v_0\|$ grows exponentially with n , Corollary 1 gives $\chi(z, v) \neq 0$ for all $v \neq 0$. Letting $\varepsilon = \frac{1}{2} - \eta$, we can either consider our system as an ε -perturbation from Cerbelli and Giona’s map, or as an η -perturbation from Arnold’s Cat map. There is subset of the parameter space $\frac{1}{3} \leq \eta < \frac{1}{8}(9 - \sqrt{33}) \approx 0.407$ in which island structures appear, splitting the parameter space into two sides. Proving (M) for the Cerbelli–Giona side follows a very similar argument to the Cat map side, but the calculations are generally more involved. For this reason, we will begin by considering the $0 < \eta < \frac{1}{3}$ perturbation and then continue with the ε -perturbation in Sect. 5.

4 Perturbation from Arnold’s Cat Map

4.1 Establishing Non-uniform Hyperbolicity

In Cerbelli and Giona (2005), a three-element ABC partition of the domain was defined with $H(A) \subset A \cup B$, $H(B) = C$, and $H(C) \subset A$. Their derivative matrix $DH|_A = DH_1$ was hyperbolic which, together with the fact that orbits leaving A

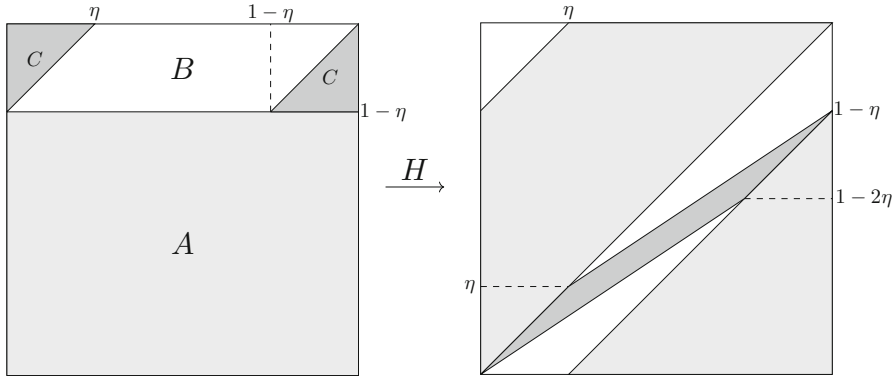


Fig. 2 Partition of the torus for H , establishing return times to A in $\{1, 2, 3\}$. Case illustrated $\eta = \frac{1}{4}$, the image of the partition is also shown with consistent shading

return after exactly two iterations in A^c , allowed Cerbelli and Giona to reduce much of the dynamics to that of a hyperbolic toral automorphism, with well-understood mixing properties.

While this approach is not possible for our family of maps, we do retain an upper bound on return times to A , illustrated by the partition of the domain given in Fig. 2. One can show that $H(A) \subset A \cup B$, $H(B) \subset A \cup C$, $H(C) \subset A$ so that orbits leaving A return after spending one or two iterations in $B \cup C$. We call the path an orbit takes around this partition its *itinerary*. Any itinerary, for example

$$AABCABAABABCA \dots$$

can be split up into itinerary blocks I_j ending in A . In the above example this would look like

$$A \ A \ BCA \ BA \ A \ BA \ BCA \dots$$

There are three¹ unique itinerary blocks

$$I_1 = A, \quad I_2 = BA, \quad I_3 = BCA,$$

with corresponding matrices

$$M_1 = DH_1, \quad M_2 = DH_1 DH_0, \quad M_3 = DH_1 DH_0^2.$$

Each M_j is hyperbolic for η strictly less than $\frac{1}{3}$, where M_3 loses hyperbolicity. Our parameter range, then, is $0 < \eta < \frac{1}{3}$.

Proposition 1 *We have nonzero Lyapunov exponents $\chi(z, v) \neq 0$ for almost every $z \in \mathbb{T}^2$, $v \neq 0$, when $0 < \eta < \frac{1}{3}$.*

¹ Four if you include CA , the first block in the itinerary of a point starting in C , but this also has corresponding matrix M_2 .

Proof Let v be a nonzero vector in the tangent space at x . As the orbit starting at x completes an itinerary block I_j , the effect on v is to premultiply by the matrix M_j . Our aim is to find a vector v_0 which sees expansion in its norm after each itinerary block. The issue we have to overcome is the possibility that expansion by one matrix may be immediately undone by contraction from another. We do this by constructing an invariant, expanding cone.

We define a cone \mathcal{C} as a subset of $\mathbb{R}^2 \setminus \{0\}$ such that if $v \in \mathcal{C}$ then $kv \in \mathcal{C}$ for any real $k \neq 0$. Given a matrix M we say that \mathcal{C} is *invariant* if $M\mathcal{C} \subset \mathcal{C}$. That is, vectors in the cone remain in the cone when premultiplied by M . We say that the cone is *expanding* if $\|Mv\| > \|v\|$ for every $v \in \mathcal{C}$, where $\|\cdot\|$ is some norm we choose to put on the tangent space. In the tangent space take coordinates $(v_1, v_2)^T \in \mathbb{R}^2$. Since the transformations we are considering are linear and cones are double sided, the gradient of a vector is the only important feature.

Starting with invariance, if the gradients g_j^u, g_j^s of the unstable, stable eigenvectors of M_j satisfy

$$g_1^s(\eta) < g_2^s(\eta) < g_3^s(\eta) < g_3^u(\eta) < g_2^u(\eta) < g_1^u(\eta),$$

then the cone bounded by (and including) the unstable eigenvectors of M_1 and M_3 will be invariant. Explicit expressions for these gradients will be given as supplementary material, and the chain of inequalities is easily verified for all $0 < \eta < \frac{1}{3}$.

It is clear, then, that it is possible to construct an invariant cone and, in fact, we have multiple options. The minimal cone is the smallest gradient range we can take to include all the unstable eigenvectors, defined at each parameter value. This will be a particularly useful construction later on as it gives good bounds on the gradients of local unstable manifolds. Its η -dependence, however, makes the expansion factor calculations quite tedious. Given that $g_3^s(\eta) < \inf_{\eta} g_3^u(\eta)$ across $0 < \eta < \frac{1}{3}$, the cone bounded by (but not including) the vectors v_{\pm} with gradients $g^+ = \sup_{\eta} g_1^u(\eta) = \frac{2}{\sqrt{5}-1}$ and $g^- = \inf_{\eta} g_3^u(\eta) = 1$ is invariant. Write this η -independent cone as $\bar{\mathcal{C}}$.

We will now show that $\bar{\mathcal{C}}$ is expanding. If across $0 < \eta < \frac{1}{3}$ each of the M_j expands both of the bounding vectors v_{\pm} , then the same holds for all vectors in the cone. To see this, note that (by hyperbolicity) M_j expands its unstable eigenvector v_u , and contracts its stable eigenvector v_s . Let $\text{ex}(v) := \frac{\|M_j v\|}{\|v\|}$, then $\text{ex}(v_u) > 1$ and $\text{ex}(v_s) < 1$. As we rotate v from v_u to v_s , we pass through one of v_{\pm} and $\text{ex}(v)$ has at most one local minimum. If $\text{ex}(v_{\pm}) > 1$, then this minimum must lie between v_{\pm} and v_s , i.e. outside of the cone, so $\{\text{ex}(v) \mid v \in \bar{\mathcal{C}}\}$ is minimal at one of its boundaries. To simplify the calculations take $\|\cdot\|$ to be the $\|\cdot\|_{\infty}$ norm then $\|(v_1, v_2)^T\| = |v_2|$ for all vectors in the cone, since within $\bar{\mathcal{C}}$ we always have $|v_2| \geq |v_1|$. Normalise the cone boundaries as $v_{\pm} = \left(\frac{1}{g^{\pm}}, 1\right)^T$, now we can calculate:

- $\|M_1(1, 1)^T\| = \frac{2\eta-3}{\eta-1} > 3$
- $\|M_2(1, 1)^T\| = \frac{3\eta^2-7\eta+3}{\eta(1-\eta)} > \frac{9}{2}$
- $\|M_3(1, 1)^T\| = 4 - \frac{10}{\eta} + \frac{3}{\eta^2} > 1$

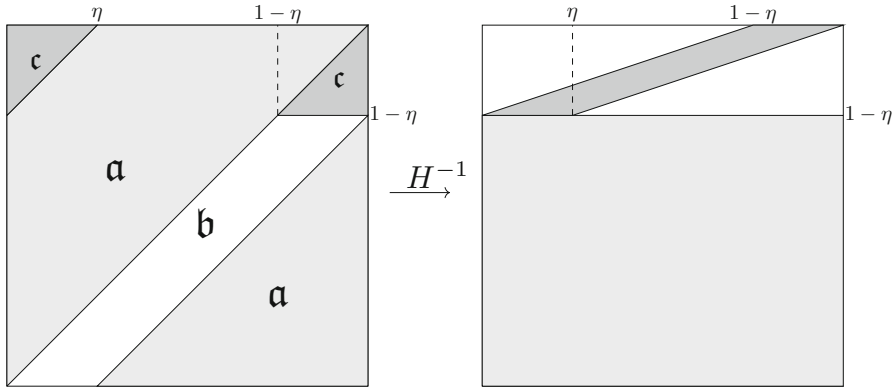


Fig. 3 A partition of the torus based on returns to a under H^{-1} and its image under H^{-1} . Case illustrated $\eta = \frac{1}{4}$

- $\|M_1 \left(\frac{\sqrt{5}-1}{2}, 1 \right)^T\| = \frac{(1+\sqrt{5})(\eta-1)-2}{2(\eta-1)} > \frac{3+\sqrt{5}}{2}$
- $\|M_2 \left(\frac{\sqrt{5}-1}{2}, 1 \right)^T\| = \frac{2\sqrt{5}\eta^2-3\sqrt{5}\eta-5\eta+6}{2\eta(1-\eta)} > \frac{39-7\sqrt{5}}{4}$
- $\|M_3 \left(\frac{\sqrt{5}-1}{2}, 1 \right)^T\| = \frac{(3\sqrt{5}-1)\eta^3-(7\sqrt{5}+7)\eta^2+(3\sqrt{5}+17)\eta-6}{2\eta^2(\eta-1)} > \frac{31-9\sqrt{5}}{4}$

for all $0 < \eta < \frac{1}{3}$, so that the cone is expanding across the parameter range. □

This establishes H as non-uniformly hyperbolic over $0 < \eta < \frac{1}{3}$. The aim of the next section is to show that **(M)** holds, establishing ergodicity.

4.2 Establishing ergodicity

Return time partitions and invariant cones can be similarly constructed for H^{-1} . These are useful for the next step, so we will give them now. Figure 3 shows the partition for returns to the set a . The itinerary blocks are follow the same pattern: a , ba , and bca , with corresponding matrices \mathfrak{M}_1 , \mathfrak{M}_2 , and \mathfrak{M}_3 , respectively. The eigenvectors of each of these matrices allow us to construct an invariant expanding cone \mathcal{C}' . Let $\mathfrak{g}_j^s(\eta)$, $\mathfrak{g}_j^u(\eta)$ be the gradients of the stable, unstable eigenvectors of \mathfrak{M}_j . One can verify that

$$\mathfrak{g}_1^u(\eta) < \mathfrak{g}_2^u(\eta) < \mathfrak{g}_3^u(\eta) < \mathfrak{g}_3^s(\eta) < \mathfrak{g}_2^s(\eta) < \mathfrak{g}_1^s(\eta)$$

for $0 < \eta < \frac{1}{3}$ so that we can take our minimal backwards cone to be the cone bounded by (and containing) the unstable eigenvectors of \mathfrak{M}_1 and \mathfrak{M}_3 . As before, taking the union of these cones over $0 < \eta < \frac{1}{3}$ gives an η -independent invariant expanding cone $\overline{\mathcal{C}'}$ for H^{-1} .

We may define local stable and unstable manifolds at any point z where we have nonzero Lyapunov exponents. These are line segments aligned with the subspace E_z^s as defined in Theorem 3, taking $f = H$ to find the stable direction, and $f = H^{-1}$ to

find the unstable direction. The following lemma provides bounds on the gradients of these line segments.

Lemma 1 *Given local unstable, stable manifolds $\gamma_u(z), \gamma_s(z)$ at $z \in X'$, let m_0, n_0 be the smallest non-negative integers such that $H^{m_0}(z) \in H(A), H^{-n_0}(z) \in H^{-1}(a)$. Then,*

- $H^{m_0}(\gamma_u(z))$ contains a segment γ aligned with some vector $v \in \mathcal{C}$,
- $H^{-n_0}(\gamma_s(z))$ contains a segment γ' aligned with some vector $v' \in \mathcal{C}'$.

Proof We first note the link between the two minimal cones. Let $v_u(M_j), v_s(M_j)$ be vector subspaces generated by the unstable and stable eigenvectors of some hyperbolic matrix M_j . Clearly $v_u(M_1) = v_s(M_1^{-1}) = v_s(\mathfrak{M}_1)$ and, in fact, we can always relate the stable, unstable eigenvectors of M_j to the unstable, stable eigenvectors of \mathfrak{M}_j . For $j = 2, 3$ these are given by

$$v_s(M_j) = DH_1 v_u(\mathfrak{M}_j) \tag{3}$$

and

$$v_u(M_j) = DH_1 v_s(\mathfrak{M}_j). \tag{4}$$

To see this, note that in the $j = 2$ case:

$$\begin{aligned} M_2^{-1} \cdot DH_1 v_u(\mathfrak{M}_2) &= DH_0^{-1} DH_1^{-1} \cdot DH_1 v_u(\mathfrak{M}_2) \\ &= \left(DH_1 DH_1^{-1} \right) DH_0^{-1} v_u(\mathfrak{M}_2) \\ &= DH_1 \mathfrak{M}_2 v_u(\mathfrak{M}_2) \\ &= c DH_1 v_u(\mathfrak{M}_2) \end{aligned}$$

for some c with $|c| > 1$. This implies $DH_1 v_u(\mathfrak{M}_2)$ is in the stable subspace of M_2 , showing (3). The same argument applied to the right hand side of (4) yields $|c| < 1$ as required. The case $j = 3$ is analogous.

Now let $\gamma_u(z)$ be the local unstable manifold at some $z \in X'$. By the partition construction, m_0 is in $\{0, 1, 2\}$. Now $H^{m_0}(\gamma_u(z))$ is a piecewise linear curve, the union of at most 3 line segments γ_j . Since z lies outside of the singularity set S , $H^{m_0}(z)$ lies in the interior of some γ_j , call it γ .

By definition, for any $\zeta, \zeta' \in \gamma_u(z)$

$$\text{dist}(H^{-n}(\zeta), H^{-n}(\zeta')) \rightarrow 0$$

as $n \rightarrow \infty$. By extension we have that

$$\text{dist}(H^{-n}(\xi), H^{-n}(\xi')) \rightarrow 0 \tag{5}$$

for any $\xi, \xi' \in \gamma$.

This means that $H^{-1}(\gamma) \subset H^{-1}(\mathfrak{a})$ must be aligned with some vector in the cone region \mathcal{C}_s bounded by $v_s(\mathfrak{M}_1)$ and $v_s(\mathfrak{M}_3)$, which includes $v_s(\mathfrak{M}_2)$.² For if it falls outside of this region, it will be pulled into the invariant expanding cone $\overline{\mathcal{C}'}$ for H^{-1} , which contradicts (5). Now if we apply H to $H^{-1}(\gamma) \subset A$, γ must align with a vector in $DH_1 \mathcal{C}_s$. By (4), this is precisely the minimal cone for H . The argument for local stable manifolds is analogous, instead using (3). \square

The main result of this section is the following.

Proposition 2 *Condition (M) holds for H when $0 < \eta < \eta_1 \approx 0.324$.*

We will use the known behaviour of returns to $H(A)$ (resp. $H^{-1}(\mathfrak{a})$), and expansion during this return, to grow the images of local manifolds to the point where an intersection is certain in $A_1 = H(A) \cap H^{-1}(\mathfrak{a})$. This is a quadrilateral, shown in Fig. 4. We call any line segment in A_1 which joins its upper and lower boundaries a v -segment. Similarly we call any line segment in A_1 which joins its left and right (sloping) boundaries a h -segment. Clearly v - and h -segments must always intersect. Given $z, z' \in X'$ our aim, then, is to find m, n such that $H^m(\gamma_u(z))$ contains a v -segment and $H^{-n}(\gamma_s(z'))$ contains a h -segment.

The key issue we have to overcome in the growth stage is that while the images of the segments may grow exponentially in total length, the sign alternating property (as described in Cerbelli and Giona 2005) means that they can repeatedly double back on themselves, meaning that their total diameter (be this in the x or y directions) does not necessarily grow. When considering unstable manifolds, we define the *diameter* of a line segment Γ as $\text{diam}(\Gamma) = \nu(\{y \mid (x, y) \in \Gamma\})$, where ν is the Lebesgue measure on \mathbb{R} . When considering stable manifolds, we instead define diameter using the projection to the x -axis.

We start with the method for growing unstable manifolds, partitioning $\mathfrak{a} = H(A)$ into three sets \mathfrak{a}_i , where the subscript i is the return time of its elements to \mathfrak{a} . This is shown in Fig. 4. We say that a line segment has *non-simple intersection* with \mathfrak{a}_i if its restriction to \mathfrak{a}_i contains more than 1 connected component. The growth stage involves iteratively applying the following lemma.

Lemma 2 *Let Γ_{p-1} be a line segment satisfying*

- (C1) $\Gamma_{p-1} \subset \mathfrak{a}$,
- (C2) Γ_{p-1} is aligned with some vector in the minimal invariant cone \mathcal{C} for H ,

and which has simple intersection with each of the \mathfrak{a}_i . There exists a line segment Γ_p satisfying (C1), (C2),

- (C3) $\Gamma_p \subset H^i(\Gamma_{p-1})$ for a chosen $i \in \{1, 2, 3\}$, and
- (C4) There exists $\delta > 0$ such that $\text{diam}(\Gamma_p) \geq (1 + \delta) \text{diam}(\Gamma_{p-1})$.

Proof The process of generating Γ_p from Γ_{p-1} is as follows. Based on the location of Γ_{p-1} in \mathfrak{a} , we will restrict Γ_{p-1} to one of the \mathfrak{a}_i then map it forwards under H^i to give Γ_p , satisfying (C3). By definition of the \mathfrak{a}_i , (C1) is satisfied. If Γ_{p-1} is aligned

² The argument for the ε -perturbation in Sect. 5 is analogous, but there the cone is bounded by $v_s(\mathfrak{M}_2)$ and $v_s(\mathfrak{M}_3)$.

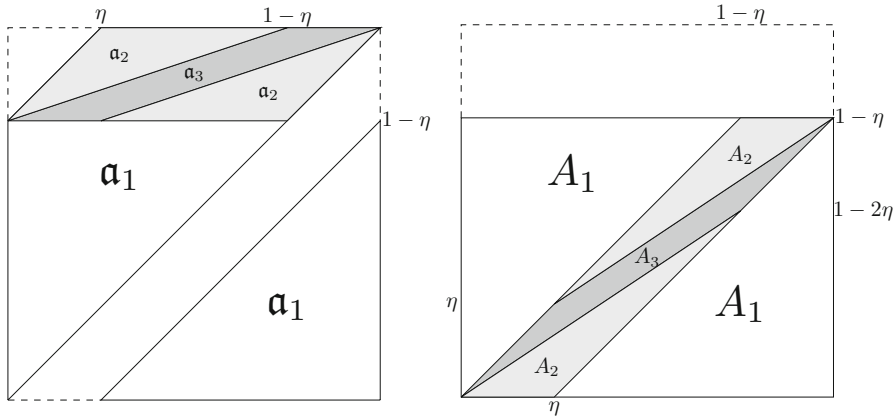


Fig. 4 Left: a partition of a into three parts a_i , where i is the return time of points in a_i to a . Right: the equivalent plot for A , considering return times under H^{-1}

with some $v \in \mathcal{C}$, Γ_p is aligned with $M_i v$. By cone invariance, this is also in \mathcal{C} , so (C2) is satisfied.

The expansion in diameter can be bounded from below by

$$K_i(\eta) = \inf_{v \in \mathcal{C}} \frac{\|M_i v\|}{\|v\|}$$

where, again, we are using the $\|\cdot\|_\infty$ norm. Since we have already shown that the cone is expanding, if Γ_{p-1} is entirely contained within some a_i then taking $\Gamma_p = H^i(\Gamma_{p-1})$ ensures expansion in diameter. Where it becomes more interesting is when Γ_p intersects multiple a_i . Looking at each of the M_i across the invariant cone, at every parameter value M_1 has the smallest expansion on its eigenvector $v_u(M_1)$, M_2 and M_3 have the smallest expansion on the other cone boundary $v_u(M_3)$. Letting λ_i be the magnitude of the unstable eigenvalue of M_i , K_1 and K_3 are given by

$$K_1(\eta) = \lambda_1(\eta) = \frac{3 - 2\eta + \sqrt{5 - 4\eta}}{2(1 - \eta)}$$

and

$$K_3(\eta) = \lambda_3(\eta) = \frac{3 - 9\eta + 2\eta^2 + \sqrt{-36\eta^3 + 93\eta^2 - 54\eta + 9}}{2\eta^2}.$$

Next

$$K_2(\eta) = \frac{2\eta - 3}{1 - \eta} \frac{1}{g_3^u(\eta)} + \frac{3 - \eta}{\eta},$$

calculated using the lower elements of M_2 , the unit vector $\left(\frac{1}{s_3}, 1\right)^T$, and the fact that M_2 reverses the orientation of vectors in the cone.

Throughout, we assume that Γ_{p-1} has simple intersection with each of the α_i . Suppose Γ_{p-1} intersects α_1 and α_2 , and write its restriction to these sets as Γ^1 and Γ^2 , respectively. Since $K_1(\eta)$ and $K_2(\eta)$ are both greater than 2 for all $0 < \eta < \frac{1}{3}$, and one of Γ^1, Γ^2 has diameter greater than or equal to $\frac{1}{2}$, we can restrict to that segment Γ^i and expand under H^i to establish that Γ_p has larger diameter than Γ_{p-1} . Now suppose Γ_{p-1} intersects α_1 and α_3 . If the proportion of the diameter of Γ_{p-1} in α_1 is greater than $\frac{1}{K_1(\eta)}$, we can simply expand from there. Otherwise Γ^3 has diameter greater than or equal to $1 - \frac{1}{K_1(\eta)}$, and we can expand from α_3 provided that

$$K_3(\eta) > \frac{1}{1 - \frac{1}{K_1(\eta)}}.$$

The above is satisfied for approximately $\eta < 0.332$. The case where Γ_{p-1} intersects α_2 and α_3 is similar and does not further restrict the parameter range.

Now suppose Γ_{p-1} intersects α_1, α_2 , and α_3 . By the same argument as before, we require

$$K_3(\eta) > \frac{1}{1 - \frac{1}{K_1(\eta)} - \frac{1}{K_2(\eta)}}.$$

Solving this numerically, the above inequality is satisfied for approximately $\eta < 0.327$. In any case, then, (C4) is satisfied. □

The method for growing the backwards images of local stable manifolds is entirely analogous. We divide up $A = H^{-1}(a)$ into A_1, A_2, A_3 based on return time to A under H^{-1} (see Fig. 4). The relevant hyperbolic matrices associated with the return map are \mathfrak{M}_i , which share an invariant, expanding cone C' . We make minor adjustments to the (C) conditions to give:

Lemma 3 *Let Γ_{p-1} be a line segment satisfying*

(C1') $\Gamma_{p-1} \subset A$,

(C2') Γ_{p-1} is aligned with some vector in the minimal invariant cone C' for H^{-1} ,

and which has simple intersection with each of the A_i . There exists a line segment Γ_p satisfying (C1'), (C2'),

(C3') $\Gamma_p \subset H^{-i}(\Gamma_{p-1})$ for a chosen $i \in \{1, 2, 3\}$,

(C4') There exists $\delta > 0$ such that $\text{diam}(\Gamma_p) \geq (1 + \delta) \text{diam}(\Gamma_{p-1})$,

where we measure the diameter of a line segment using its projection to the x -axis.

Proof As before, define

$$\mathcal{K}_i(\eta) = \inf_{v \in C'} \frac{\|\mathfrak{M}_i v\|}{\|v\|}.$$

All of the \mathfrak{M}_i see their minimum cone expansion on the cone boundary given by the unstable eigenvector of \mathfrak{M}_3 . The key calculation we have to make is the parameter value η_1 such that

$$\mathcal{K}_3(\eta) > \frac{1}{1 - \frac{1}{\kappa_1(\eta)} - \frac{1}{\kappa_2(\eta)}} \tag{6}$$

for $0 < \eta < \eta_1$. We can solve numerically, giving $\eta_1 \approx 0.324$. □

Both of these lemmas hold, then, provided that $0 < \eta < \eta_1$. They ensure the exponential growth in diameter of the segments Γ_p up to some Γ_P which has non-simple intersection with some α_i (or A_i for the stable case). At this point we will map directly into v - and h -segments.

Lemma 4 *For any line segment $\Gamma_P \subset \mathfrak{a}$ which is aligned with a vector in \mathcal{C} and has non-simple intersection with some α_i , $H^k(\Gamma_P)$ contains a v -segment for some $k \in \{0, 3, 5\}$.*

Proof All non-simple intersections give useful geometric information about Γ_P . Suppose it has non-simple intersection with α_3 . Then, as a connected straight line segment, it must *traverse* α_1 , that is, it connects the upper and lower boundaries of α_1 , passing through α_1 . By definition, this Γ_P contains a v -segment. Now suppose Γ_P has non-simple intersection with α_2 . It follows that Γ_P traverses α_1 (v -segment) or Γ_P traverses α_3 , connecting its sloping boundaries. This is case (I). We will show that any such segment contains a v -segment in its 5th image. Finally, assume that Γ_P has non-simple intersection with α_1 . It follows that we traverse α_3 , case (I), or the restriction to α_2 is sufficiently large that its 3rd image contains a v -segment, case (II).

We will start by showing case (I). Consider the quadrilateral $\mathcal{Q}_3 \subset \mathfrak{a}_3$, defined by the four points P_j , shown in Fig. 5. Explicit coordinates for each of these points are given as part of the supplementary material. All of the points in the interior of \mathcal{Q}_3 share the same itinerary path under 5 iterations of H , $BCAAA$, so $H^5(\mathcal{Q}_3)$ is also a quadrilateral and any straight line segment contained within \mathcal{Q}_3 maps into a new straight line segment under H^5 . It is clear that any Γ_P which traverses α_3 , joining its sloping boundaries, must also traverse \mathcal{Q}_3 . The sloping boundaries of \mathcal{Q}_3 map into the upper and lower boundaries of α_1 under H^5 , so if Γ_P connects these sloping boundaries, $H^5(\Gamma_P)$ contains a v -segment.

Case (II) can be argued similarly. We assume that Γ_P has non-simple intersection with α_1 and that we do not traverse α_3 in such a way that we can argue as in case (I). We will concentrate first on the left portion of α_2 ; we shall soon see that the analysis for the right portion is analogous.

Since we assume Γ_P does not connect the sloping sides of α_3 , it must intersect the α_1, α_3 boundary on L , shown in Fig. 6. The solid thick line shown is aligned with clockwise bound on the invariant cone, with gradient g_3^u . The intersection of Γ_P with the α_3, α_2 boundary must lie in L^* , whose x -range is bounded above by x^* .

Let Γ be the restriction to α_2 . We will show that Γ , constrained by the x^* , intersects a quadrilateral whose image under H^3 stretches across α_1 in much the same way we saw in case (I). For $\eta \leq \eta_0 = 1 - \frac{1}{\sqrt{2}} \approx 0.293$, such a quadrilateral \mathcal{Q}_2 exists and has

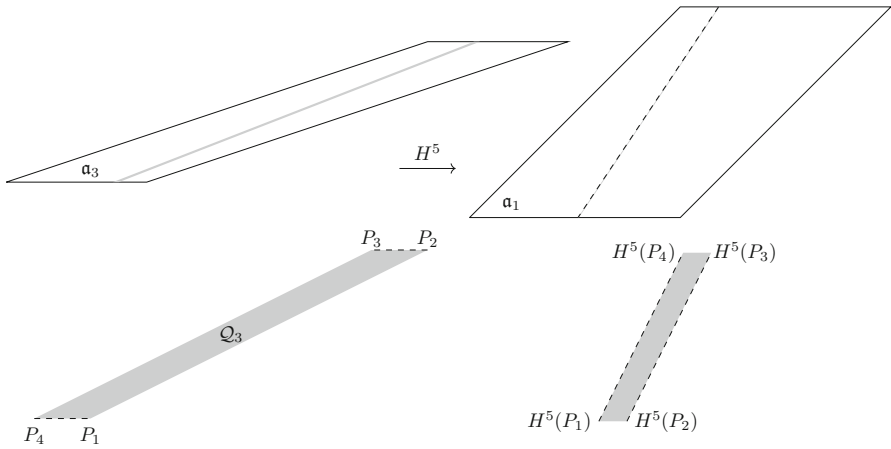


Fig. 5 Case (I). A quadrilateral $Q_3 \subset \alpha_3$ and its image in α_1 under H^5 . Any line segment Γ which joins the sloping boundaries of α_3 will join the sloping boundaries of Q_3 , and hence $H^5(\Gamma \cap Q_3)$ is a v -segment

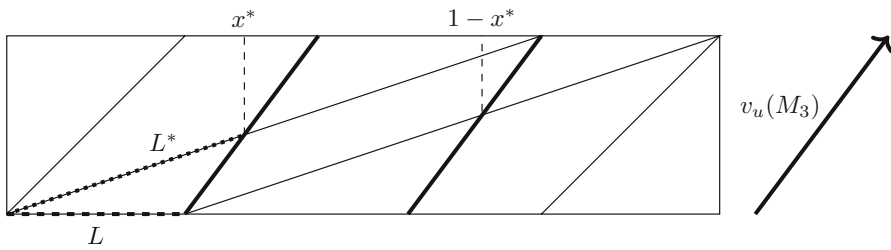


Fig. 6 Geometry of line segments satisfying case (II)

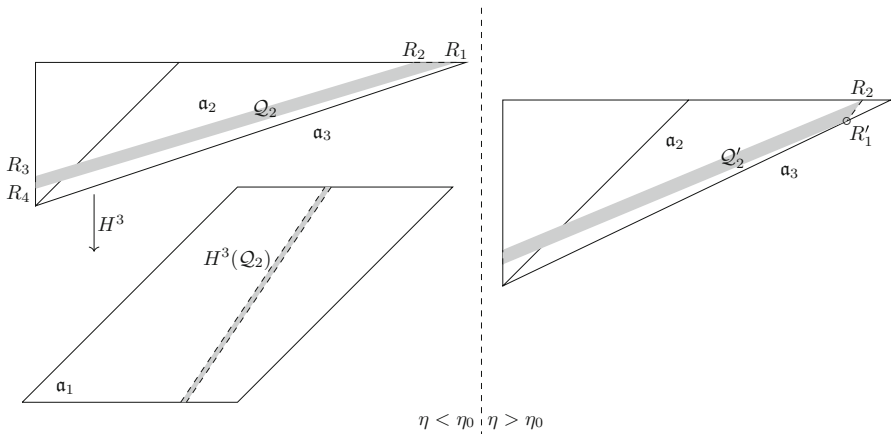


Fig. 7 Case (II) for η either side of the critical value $\eta_0 = 1 - \frac{1}{\sqrt{2}}$

all four corners on the lines $x = 0, y = 1$ (see left hand side of Fig. 7). Starting with the top-right and cycling anti-clockwise, these corners have coordinates

$$R_1 = \left(\frac{-\eta^3 + 7\eta^2 - 13\eta + 7}{3\eta^2 - 10\eta + 8}, 1 \right), \quad R_2 = \left(\frac{2(2\eta^2 - 5\eta + 3)}{3\eta^2 - 10\eta + 8}, 1 \right),$$

$$R_3 = \left(0, \frac{5\eta^2 - 13\eta + 8}{\eta^2 - 7\eta + 8} \right), \quad \text{and } R_4 = \left(0, \frac{-\eta^3 + 7\eta^2 - 14\eta + 8}{\eta^2 - 7\eta + 8} \right).$$

Any line segment joining the a_2, a_3 boundary to the a_2, a_1 boundary must connect the parallel boundaries of Q_2 and therefore maps into a v -segment. At the critical value $\eta = \eta_0$ the point R_1 lies on the rightmost corner of $a_2, (1 - \eta, 1)$. Now let $\eta > \eta_0$ and consider the quadrilateral Q'_2 defined by the corners R_2, R_3, R_4 , and

$$R'_1 = (x', y') = \left(\frac{-\eta^2 + 2\eta - 1}{\eta(2\eta - 3)}, \frac{-2\eta^2 + 6\eta - 4}{2\eta - 3} \right). \tag{7}$$

This final corner also maps into $y = 1 - \eta$ under H^3 ; hence, any line segment which joins the parallel sides of Q'_2 maps into a v -segment. Certainly if $x^*(\eta) < x'(\eta)$ for $\eta_0 < \eta < \eta_1$, then Γ will connect the parallel sides of Q'_2 . First, we solve line equations to give

$$x^*(\eta) = \frac{\eta g_3^u(\eta)}{g_3^u(\eta) - \frac{\eta}{1-\eta}}$$

which is bounded from above by $x^*(\eta_1) \approx 0.5512$. Next by (7),

$$x'(\eta) = \frac{-\eta^2 + 2\eta - 1}{\eta(2\eta - 3)}$$

which is bounded from below by $x'(\eta_1) \approx 0.5998$, establishing the result.

The case where Γ traverses the other (right) part of a_2 is analogous. Note that we can transform one part of a_2 into the other by reflecting in the lines $y = 1 - \frac{\eta}{2}$ and $x = \frac{1}{2}$,³ written as $(S_x \circ S_y)(a_2) = a_2$. Now the images of Q_2 and Q'_2 under $S_x \circ S_y$ span across the right portion of a_2 in an analogous fashion to before and also map into v -segments under H^3 . Making the same assumption as before, that case (II) holds but case (I) does not, we know that Γ intersects the a_2, a_3 boundary at some point (x, y) with $x > 1 - x^*$ (see Fig. 6). To ensure that Γ connects the parallel sides of $(S_x \circ S_y)(Q'_2)$, it remains to check that the x -coordinate of $(S_x \circ S_y)(x', y'), 1 - x'$, is strictly less than $1 - x^*$ across $\eta_0 < \eta < \eta_1$. Indeed, $1 - x'(\eta) < 1 - x^*(\eta)$ follows from $x^*(\eta) < x'(\eta)$, established in the previous case. \square

Lemma 5 *For any line segment $\Gamma_P \subset A$ which is aligned with a vector in \mathcal{C}' and has non-simple intersection with some $A_i, H^{-k}(\Gamma_P)$ contains a h -segment for some $k \in \{0, 3, 5\}$.*

³ Since the lines are orthogonal, $S_x \circ S_y = S_y \circ S_x$.

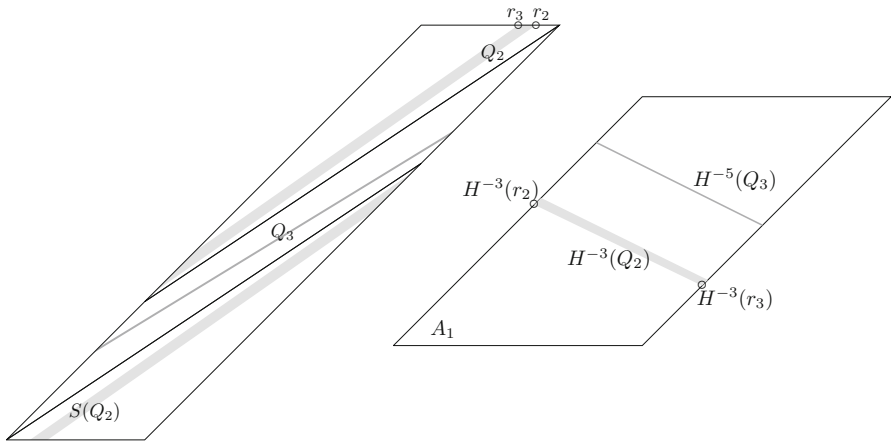


Fig. 8 Two quadrilaterals $Q_2 \subset A_2$ and $Q_3 \subset A_3$ which map into A_1 under H^{-3} and H^{-5} , respectively. Their long boundaries map into the sloping boundaries of A_1 , so segments Γ which join these long boundaries map into h -segments. Case illustrated $\eta = \frac{1}{4}$

Proof The argument is similar to the forwards-time case. A partition of $H^{-1}(a) = A$ by return time is shown in Fig. 4. Case (I) assumes that Γ connects the two A_2, A_3 boundaries through A_3 , case (II) assumes that Γ joins the two sloping boundaries of A_1 through $A_2 \cup A_3$, but that case (I) does not hold. We will show that in case (I) $H^{-5}(\Gamma)$ contains a h -segment, and in case (II) $H^{-3}(\Gamma)$ contains a h -segment. Starting with Γ satisfying case (I), Fig. 8 shows a quadrilateral $Q_3 \subset A_3$ with two short sides on the A_1, A_3 boundaries. It follows that Γ must connect a segment which joins the longer sides of Q_3 , through Q_3 . The argument is now the same as in the forwards time analysis, all points in Q_3 share the same itinerary under 5 iterations of H^{-1} , $bcaaa$, so $H^{-5}(Q_3)$ is a quadrilateral in A . One can verify that it is wholly contained in $A_1 \subset A$ and that its longer sides map into its sloping boundaries (see right image in Fig. 8). $H^{-5}(\Gamma)$ then contains a segment which connects these two boundaries through A_1 , that is, $H^{-5}(\Gamma)$ contains a h -segment. Explicit expressions for the corner coordinates of Q_3 and their images under H^{-5} will be given as supplementary material.

Moving onto Γ satisfying case (II) and first focusing on the upper portion of A_2 , for $\eta \leq \eta_0$ we can follow the same argument, defining a quadrilateral $Q_2 \subset A_2$ with itinerary baa and $H^{-3}(Q_2) \subset A_1$ (see Fig. 8). Its long sides must be joined by Γ and map into the boundary of A_1 , so $H^{-3}(\Gamma)$ contains a h -segment. Starting with the bottom corner of Q_2 nearest the A_2, A_3 boundary and cycling anti-clockwise, label these points as r_1, \dots, r_4 , which have coordinates

$$r_1 = \left(\frac{\eta^3 - 4\eta^2 + 3\eta + 1}{3\eta^2 - 10\eta + 8}, \frac{\eta^3 - 4\eta^2 + 3\eta + 1}{3\eta^2 - 10\eta + 8} \right),$$

$$r_2 = \left(\frac{5\eta^3 - 20\eta^2 + 24\eta - 8}{4\eta^3 - 18\eta^2 + 23\eta - 8}, 1 - \eta \right),$$

$$r_3 = \left(\frac{-\eta^4 + 8\eta^3 - 23\eta^2 + 25\eta - 8}{4\eta^3 - 18\eta^2 + 23\eta - 8}, 1 - \eta \right), \text{ and}$$

$$r_4 = \left(\frac{2 - \eta^2}{3\eta^2 - 10\eta + 8}, \frac{2 - \eta^2}{3\eta^2 - 10\eta + 8} \right).$$

For $\eta > \eta_0$ we consider the quadrilateral Q'_2 with corners r_2, r_3, r_4 and

$$r'_1 = \left(\frac{3\eta^2 - 5\eta + 1}{\eta(2\eta - 3)}, \frac{-2\eta^3 + 7\eta^2 - 6\eta + 1}{\eta(2\eta - 3)} \right).$$

This is shown in Fig. 9, with the x -coordinate of r'_1 highlighted as $x'(\eta)$. Like in the forwards-time case, we need to check that $x'(\eta)$ is not so far along the A_2, A_3 boundary that any Γ satisfying case (II) does not connect the parallel sides of Q'_2 . Letting $\mathfrak{g}_3^u(\eta)$ be the gradient of the anti-clockwise invariant cone boundary for H^{-1} , this amounts to showing that $x'(\eta) < x^*(\eta)$ where (x^*, y^*) lies on the intersection of the lines

$$y = \eta + \frac{1 - 2\eta}{1 - \eta}(x - \eta)$$

(the A_2, A_3 boundary) and

$$y = 1 - 2\eta + \mathfrak{g}_3^u(\eta)(x - 1 + \eta),$$

shown as the solid bold line in Fig. 9. Solving for x gives

$$x^*(\eta) = \frac{\eta^2 + 3\eta - 1 + \mathfrak{g}_3^u(\eta)(1 - \eta)^2}{\mathfrak{g}_3^u(\eta)(1 - \eta) - 1 + 2\eta}.$$

One can now verify that $x'(\eta) < x'(\eta_1) < x^*(\eta_1) < x^*(\eta)$ for all $\eta_0 < \eta < \eta_1$, establishing the result. To conclude case (II) we must extend the analysis to the other portion of A_2 . This process is entirely analogous to the forwards-time case, taking reflections in $x = \frac{1}{2}$ and $y = \frac{1}{2} - \frac{\eta}{2}$. An example is shown in Fig. 8, with the image of Q_2 under these reflections shown as $S(Q_2)$. □

We are now ready to prove Proposition 2.

Proof of Proposition 2 Let $\gamma_u(z)$ be the local unstable manifold at some $z \in X'$. Let $m_0 \geq 0$ be the smallest integer such that $H^{m_0}(z) \in \mathfrak{a}$. Then, by Lemma 1, $H^{m_0}(\gamma_u(z))$ contains a segment Γ_0 in \mathfrak{a} , aligned with some vector in the invariant cone \mathcal{C} . We can then iteratively apply Lemma 2 to generate a sequence of line segments with exponentially increasing diameter $(\Gamma_p)_{0 \leq p \leq P}$ with each $\Gamma_p \subset H^{m_0+m_p}(\gamma_u(z))$ for some $m_p > 0$. Since the sequence has exponentially increasing diameter, after some finite number of steps P , the line segment Γ_P must have non-simple intersection with one of the a_i . Lemma 4 then tells us that $H^k(\Gamma_P)$ contains a v -segment for some $k \in \{0, 3, 5\}$. It follows that $H^m(\gamma_u(z))$ contains a v -segment where $m = m_0 + m_P + k$. Similarly given $z' \in X'$, we can apply Lemmas 1, 3, and 5 to find n

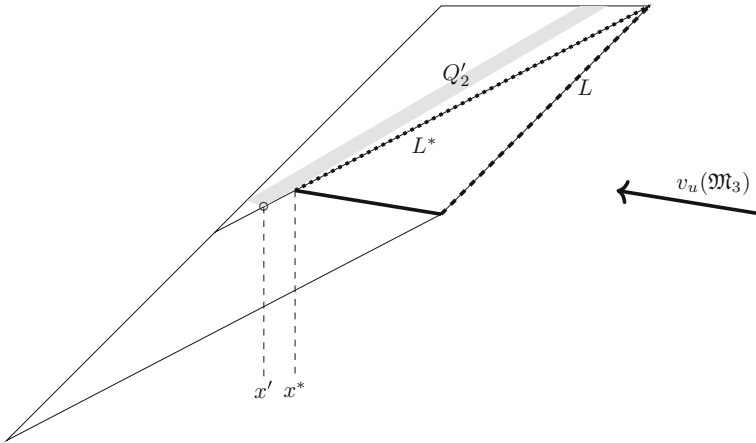


Fig. 9 Case (II) for $\eta > \eta_0$. Any Γ satisfying case (II) must intersect the A_1A_3 boundary on L and the A_2A_3 boundary on L^* . This gives a lower bound on x^* on the x -coordinate of this intersection so that if $x^* > x'$, then Γ joins the parallel sides of Q'_2

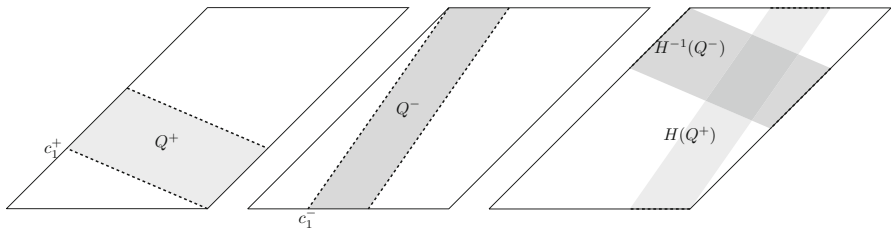


Fig. 10 Two quadrilaterals Q^+, Q^- in A_1 which map into A_1 under H and H^{-1} , respectively. Any v -segment must join the dotted sides of Q^+ and hence maps into another v -segment. Similar for h -segments and Q^-

such that $H^{-n}(\gamma_s(z'))$ contains a h -segment. Since z and z' were arbitrary, condition **(M)** holds. □

This establishes H as ergodic over $0 < \eta < \eta_1$. Stronger mixing properties can now be easily shown.

4.3 Establishing the Bernoulli Property

Proposition 3 Condition **(MR)** holds for H when $0 < \eta < \eta_1 \approx 0.324$.

Proof To establish **(MR)**, it is sufficient to show that the image of a v -segment under H contains a v -segment, and the image of a h -segment under H^{-1} contains a h -segment. We can approach this is same way as before, defining quadrilaterals which these segments must traverse and looking at their images. Define the quadrilateral Q^+

by the corners (starting from the leftmost and cycling anti-clockwise)

$$c_1^+ = \left(\frac{1 + \eta - \eta^2}{3 - 2\eta}, \frac{(1 - \eta)^2}{3 - 2\eta} \right), c_2^+ = (0, 0),$$

$$c_3^+ = \left(\frac{(1 - \eta)^2}{3 - 2\eta}, \frac{(1 - \eta)^2}{3 - 2\eta} \right), \text{ and } c_4^+ = \left(\frac{2 - \eta}{3 - 2\eta}, \frac{2(1 - \eta)^2}{3 - 2\eta} \right).$$

This is shown in the first diagram in Fig. 10; note that we have shifted the domain horizontally to more easily see A_1 as a quadrilateral. Any v -segment must join the dotted sides of Q^+ , which map into the upper and lower boundaries of A_1 , so v -segments map into v -segments. We can similarly define the quadrilateral Q^- by the corners (starting from the leftmost and cycling anti-clockwise)

$$c_1^- = \left(\frac{1 + \eta - \eta^2}{3 - 2\eta}, 0 \right), c_2^- = \left(\frac{2 - \eta}{3 - 2\eta}, 0 \right),$$

$$c_3^- = \left(\frac{(1 - \eta)^2}{3 - 2\eta}, 1 - \eta \right), \text{ and } c_4^- = (0, 1 - \eta).$$

Again, h -segments must connect the dotted sides of Q^- , which map into the sloping boundaries of A_1 ; hence, h -segments map into h -segments. □

5 Perturbation from Cerbelli & Giona’s Map

5.1 Establishing Non-uniform Hyperbolicity

Let $\varepsilon = \frac{1}{2} - \eta$. Our method for establishing nonzero Lyapunov exponents almost everywhere for H as an ε -perturbation is essentially the same as in Sect. 4.1.

Proposition 4 *We have nonzero Lyapunov exponents $\chi(z, v) \neq 0$ for almost every $z \in \mathbb{T}^2, v \neq 0$, when $0 < \varepsilon < \varepsilon_1 \approx 0.0931$.*

Proof The partition and possible itinerary paths I_j around the partition are the same as before. Define the corresponding matrices M_j using the derivative matrices

$$DH_0 = \begin{pmatrix} 1 & \frac{-2}{1-2\varepsilon} \\ 1 & \frac{-1-2\varepsilon}{1-2\varepsilon} \end{pmatrix} \text{ and } DH_1 = \begin{pmatrix} 1 & \frac{2}{1+2\varepsilon} \\ 1 & \frac{3+2\varepsilon}{1+2\varepsilon} \end{pmatrix}.$$

Again, M_3 is the matrix which dictates our parameter range. It is hyperbolic for $\varepsilon < \varepsilon_1$, where $\varepsilon_1 = \frac{\sqrt{33}-5}{8} \approx 0.0931$. M_2 is hyperbolic for ε strictly greater than 0.

Following the same argument as in Sect. 4.1, it remains to define an invariant cone and show that it is expanding. Defining g_j^u and g_j^s as before, one can verify that

$$g_3^s(\varepsilon) < g_1^s(\varepsilon) < g_2^s(\varepsilon) < g_2^u(\varepsilon) < g_1^u(\varepsilon) < g_3^u(\varepsilon)$$

for $0 < \varepsilon < \frac{1}{\sqrt{3}} - \frac{1}{2} \approx 0.0774$, and

$$g_1^s(\varepsilon) < g_2^s(\varepsilon) < g_2^u(\varepsilon) < g_1^u(\varepsilon) < g_3^u(\varepsilon) < g_3^s(\varepsilon)$$

for $\frac{1}{\sqrt{3}} - \frac{1}{2} < \varepsilon < \varepsilon_1$. Hence, the cone \mathcal{C} , bounded by and including the unstable eigenvectors of M_2 and M_3 , is the minimal invariant cone. The common cone $\bar{\mathcal{C}}$ is then defined as the open region bounded by the unstable eigenvector of M_2 at $\varepsilon = 0$ and the unstable eigenvector of M_3 at $\varepsilon = \varepsilon_1$. Under the $\|\cdot\|_\infty$ norm, these are the unit vectors $(1, 1)^T$ and $\left(\frac{\sqrt{33}-3}{6}, 1\right)^T$, respectively. One can show that

- $\|M_1(1, 1)^T\| > \frac{\sqrt{33}+9}{4}$
- $\|M_2(1, 1)^T\| > 1$
- $\|M_3(1, 1)^T\| > \frac{9+\sqrt{33}}{6}$
- $\|M_1\left(\frac{\sqrt{33}-3}{6}, 1\right)^T\| > \frac{9+5\sqrt{33}}{12}$
- $\|M_2\left(\frac{\sqrt{33}-3}{6}, 1\right)^T\| > 7 - \frac{2\sqrt{33}}{3}$
- $\|M_3\left(\frac{\sqrt{33}-3}{6}, 1\right)^T\| > 1$

for all ε in our range, so that our cone is expanding. □

This establishes non-uniform hyperbolicity. As before, the next section shows ergodicity.

5.2 Establishing Ergodicity

Proposition 5 *Condition (M) holds for H over $\varepsilon_0 < \varepsilon \leq \varepsilon_2$, where $\varepsilon_0 \approx 0.00925$ and $\varepsilon_2 \approx 0.0850$.*

The overall method for establishing (M) is unchanged. The key constructions are the partitions of $H(A)$ and $H^{-1}(a)$ given in Sect. 4.2, and the invariant cones \mathcal{C} for H (given above) and \mathcal{C}' for H^{-1} . Defining the \mathfrak{M}_j as before, \mathcal{C}' is defined at each ε as the cone bounded by (and including) the unstable eigenvectors of \mathfrak{M}_2 and \mathfrak{M}_3 , i.e. the nonzero vectors with gradient $g_3^u < g < g_2^u$. One can show (by the same method as before) that \mathcal{C}' is invariant and expanding.

For the sake of brevity, we will only describe the process of growing the backwards images of local stable manifolds. The process for unstable manifolds is entirely analogous and, due to \mathcal{C} covering a smaller gradient range than \mathcal{C}' , results in less stringent bounds on the parameter range.

While for the η -perturbation the growth stage was relatively straightforward and the h -segment mappings more involved, the opposite is true for the ε -perturbation. If we were to follow the same method as before, reducing the parameter range to satisfy equations like (6), we would be left with just a fragment of the parameter range. Our way around this necessitates growing piecewise linear curves rather than line segments. To ensure that we can find the diameter of a curve by summing the diameters of its

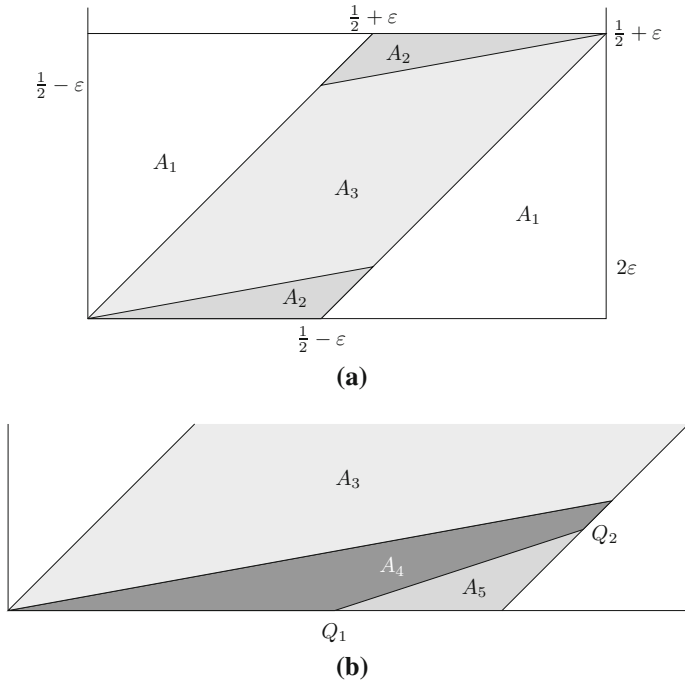


Fig. 11 Part **a** gives partition of A based on return time to A under iterations of H^{-1} . Part **b** shows a subdivision $A_4 \cup A_5 = A_2$, with the boundary between these sets defined as the segment joining the points Q_1, Q_2 . Case illustrated $\varepsilon = 0.05$

constituent line segments, we require that a curve *does not double back on itself*, that is, the projection to the x -axis is injective. The lemma for the growth stage is as follows:

Lemma 6 *Let Γ_{p-1} be a piecewise linear curve satisfying*

- (C0') Γ_{p-1} *does not double back on itself,*
- (C1') $\Gamma_{p-1} \subset A$,
- (C2') *Each line segment in Γ_{p-1} is aligned with some vector in the minimal invariant cone C' for H^{-1} ,*

and which has simple intersection with each of the A_i . There exists a piecewise linear curve Γ_p satisfying (C0'), (C1'), (C2'),

- (C3') $\Gamma_p \subset H^{-i}(\Gamma_{p-1})$ *for a chosen $i \in \{1, 2, 3\}$,*
- (C4') *There exists $\delta > 0$ such that $\text{diam}(\Gamma_p) \geq (1 + \delta) \text{diam}(\Gamma_{p-1})$,*

where we measure the diameter of a curve using its projection to the x -axis.

Proof Figure 11a shows the return time partition of $A = H^{-1}(a)$ under H^{-1} . Define $\mathcal{K}_j(\varepsilon)$ for $j = 1, 2, 3$ as before. Both \mathfrak{M}_1 and \mathfrak{M}_2 see their minimum expansion over C' on the unstable eigenvector of \mathfrak{M}_2 . As does \mathfrak{M}_3 for $\varepsilon < \varepsilon^* \approx 0.07735$, then on its own unstable eigenvector for $\varepsilon > \varepsilon^*$. Since C' is expanding, each of the $\mathcal{K}_j(\varepsilon)$ are strictly greater than 1 across our parameter range.

First suppose Γ_{p-1} lies entirely within one of the A_j . Each of its constituent line segments $L(x_i, v_i)$ can be defined by an end point x_i and the vector v_i taking x_i to the other end point, with $v_i \in \mathcal{C}'$. Satisfying (C3') we let $\Gamma_p = H^{-j}(\Gamma_{p-1})$, then each $L(x_i, v_i)$ is mapped to a new segment $L(H^{-j}(x_i), \mathfrak{M}_j v_i)$ which lies in A , is aligned in \mathcal{C}' and has expanded in diameter by a factor of at least $\mathcal{K}_j(\varepsilon)$.

As the union of these new line segments, Γ_p satisfies (C1') and (C2'). It does not double back on itself since \mathfrak{M}_j will have the same orientation preserving (or reversing) effect on each of the v_i . This satisfies (C0') and tells us that the diameter of Γ_p is the sum of the diameters of the new line segments,⁴ meaning its diameter has expanded by at least the factor $\mathcal{K}_j(\varepsilon)$, satisfying (C4').

The above is the simplest case we will consider. The picture becomes more complicated as we allow intersections with multiple A_j . First assume that Γ_{p-1} intersects A_1 and one of A_2 or A_3 . We proceed by restricting to one of the A_j , $\Gamma^j := \Gamma_{p-1} \cap A_j$, and expanding from there, $\Gamma_p = H^{-j}(\Gamma^j)$. By the same reasoning given for the η -perturbation, we require

$$\mathcal{K}_2(\varepsilon) > \frac{1}{1 - \frac{1}{\mathcal{K}_1(\varepsilon)}} \tag{8}$$

and

$$\mathcal{K}_3(\varepsilon) > \frac{1}{1 - \frac{1}{\mathcal{K}_1(\varepsilon)}}. \tag{9}$$

Solving (8) gives $\varepsilon > \varepsilon_0 \approx 0.00925$, the lower bound on our parameter range. Solving (9) gives $\varepsilon < \varepsilon_3 \approx 0.0885$, slightly larger than the upper bound on our parameter range ε_2 .

Next assume that Γ_p intersects A_1, A_2 , and A_3 . The case where Γ_p intersects A_2 and A_3 but not A_1 follows as a trivial consequence and will be addressed at the end of the proof. Clearly if the proportion of the diameter in A_1 exceeds $\mathcal{K}_1(\varepsilon)^{-1}$,

$$\frac{\text{diam}(\Gamma^1)}{\text{diam}(\Gamma_{p-1})} > \frac{1}{\mathcal{K}_1(\varepsilon)},$$

then we can take $\Gamma_p = H^{-1}(\Gamma^1)$ to satisfy (C0'–5'). Otherwise we have to expand from some subset of $\Gamma^2 \cup \Gamma^3$, giving Γ_p such that

$$\text{diam}(\Gamma_p) > \frac{1}{1 - \frac{1}{\mathcal{K}_1(\varepsilon)}} \text{diam}(\Gamma^2 \cup \Gamma^3).$$

To reduce the ε dependence of the problem and simplify the equations, we will take

$$c = \sup_{\varepsilon_0 < \varepsilon \leq \varepsilon_2} \frac{1}{1 - \frac{1}{\mathcal{K}_1(\varepsilon)}} \approx 1.4765$$

⁴ Assuming it is not 1, at which point Γ_p has non-simple intersection with some A_j .

and show

$$\text{diam}(\Gamma_p) > c \text{diam}(\Gamma^2 \cup \Gamma^3). \tag{10}$$

We will give an argument for expanding Γ_{p-1} which intersects the lower portion of A_2 . The argument for the upper portion is entirely analogous due to the 180° rotational symmetry of both the partition of A and the invariant cone.

Consider the subdivision of A_2 into points which remain in A for a further iteration of H^{-1} after returning, A_4 , and those which do not, A_5 . This subdivision is shown in Fig. 11b. The labelled points are

$$Q_1 = \left(\frac{-4\varepsilon^3 - 2\varepsilon^2 + \varepsilon + \frac{1}{2}}{12\varepsilon^2 + 16\varepsilon + 1}, 0 \right) \quad \text{and} \quad Q_2 = \left(\frac{1 + 2\varepsilon}{2 + 2\varepsilon}, \frac{3\varepsilon + 2\varepsilon^2}{2 + 2\varepsilon} \right)$$

so that the segment L_1 along the A_4, A_5 boundary has gradient

$$k_1 = \frac{12\varepsilon^2 + 16\varepsilon + 1}{(2\varepsilon + 1)(2\varepsilon + 5)}.$$

The segment along the A_4, A_3 boundary has gradient

$$k_2 = \frac{4\varepsilon}{2\varepsilon + 1}.$$

Strictly speaking, at larger ε values A_4 contains an additional region in the lower part of A_5 near $(\frac{1}{2} - \varepsilon, 0)$. The only assumption we make about points in A_5 is that they return to A after two iterations, so treating this additional region as part of A_5 has no impact on our analysis.

The region A_4 has some useful properties. Firstly, like A_3 , segments contained within A_4 return to A after 3 iterations. This⁵ means we can take $\Gamma_p = H^{-3}(\Gamma_3 \cup \Gamma_4)$ and have a much larger initial curve to expand from. Secondly, diameter expansion is generally strong from A_4 . The itinerary path is baa with corresponding matrix

$$\mathfrak{M}_4 = DH_1^{-1}DH_1^{-1}DH_0^{-1}$$

which expands vectors at least as much as any of the other \mathfrak{M}_j : $\mathcal{K}_4(\varepsilon) > \mathcal{K}_j(\varepsilon)$ for all $\varepsilon_0 < \varepsilon \leq \varepsilon_2, j = 1, 2, 3$. Finally, if Γ_{p-1} intersects A_5 , then it must traverse A_4 since, by assumption, it also intersects A_3 . The case where Γ_{p-1} does not intersect A_5 is trivial, reducing to the case where Γ_{p-1} only intersects A_1 and A_3 , since A_3 and A_4 both map into A under H^{-3} and $\mathcal{K}_4 > \mathcal{K}_3$.

Assume, then, that Γ_{p-1} intersects A_5 . Let $\Gamma_p = H^{-3}(\Gamma^3 \cup \Gamma^4)$. Our aim is to minimise $\text{diam}(\Gamma_p)$, considering all possible curves Γ_{p-1} dictated by the invariant cone, and showing that it still satisfies (10). To arrive at the minimal case we can make several assumptions. Firstly, $\text{diam}(\Gamma^3) = 0$. The condition that we intersect A_3 does

⁵ Together with the fact that \mathfrak{M}_3 and \mathfrak{M}_4 have the same orientation reversing effect on the invariant cone.

not stipulate any minimum diameter in A_3 , it can be arbitrarily small. Since \mathfrak{M}_3 and \mathfrak{M}_4 have the same orientation reversing effect on vectors in the cone, assuming Γ_p does not have diameter 1 (at which point we have non-simple intersection with some A_j),

$$\text{diam}(\Gamma_p) \geq \mathcal{K}_3(\varepsilon) \text{diam}(\Gamma^3) + \mathcal{K}_4(\varepsilon) \text{diam}(\Gamma^4).$$

Comparing with (10), taking $\text{diam}(\Gamma^3) > 0$ grows the RHS of (10) by $c \text{diam}(\Gamma^3)$, but grows the LHS of (10) by at least $\mathcal{K}_3(\varepsilon)\text{diam}(\Gamma^3)$. Since $\mathcal{K}_3(\varepsilon) > c$ for every $\varepsilon_0 < \varepsilon \leq \varepsilon_2$, in the minimal case $\text{diam}(\Gamma^3) = 0$. We note that the condition (10) now looks like

$$\text{diam}(H^{-3}(\Gamma^4)) > c \text{diam}(\Gamma^4 \cup \Gamma^5),$$

which is satisfied if

$$\mathcal{K}_4(\varepsilon) > c \frac{\text{diam}(\Gamma^4) + \text{diam}(\Gamma^5)}{\text{diam}(\Gamma^4)}. \tag{11}$$

To show that this holds, we will put lower bounds on

$$\frac{\text{diam}(\Gamma^4)}{\text{diam}(\Gamma^4) + \text{diam}(\Gamma^5)} \tag{12}$$

and $\mathcal{K}_4(\varepsilon)$, then compare their product with c .

By a purely geometric argument, comparing the admissible gradients given by the invariant cone with the lines which make up the partition boundaries, we have a lower bound

$$\begin{aligned} & \frac{\text{diam}(\Gamma^4)}{\text{diam}(\Gamma^4) + \text{diam}(\Gamma^5)} \\ & > \frac{(2\varepsilon + 1)(2\varepsilon + 1 - 2k_5^+)}{(2\varepsilon + 1)(-k_4^-(2\varepsilon + 3) - k_5^+(2\varepsilon + 5)) + 12\varepsilon^2 + 16\varepsilon + 1} := \mathcal{B}_1(\varepsilon) \end{aligned}$$

where $k_5^+ = \sup_{\varepsilon} g_2^u(\varepsilon) \approx -0.08750$ and $k_4^- = \inf_{\varepsilon} g_3^u(\varepsilon) \approx -0.6688$. The calculation of this bound can be found in ‘‘Appendix’’.

We will now put a lower bound on $\mathcal{K}_4(\varepsilon)$, the minimum expansion of \mathfrak{M}_4 over the minimal cone. This is on the anti-clockwise boundary, $v_u(\mathfrak{M}_2)$, which can be described as the vector $(1, k_5(\varepsilon))^T$ with

$$k_5(\varepsilon) = \frac{\varepsilon - \sqrt{\varepsilon(4\varepsilon^2 + 5\varepsilon + 1)}}{2\varepsilon + 1} < 0.$$

By calculating the matrix entries of \mathfrak{M}_4 and noting that \mathfrak{M}_4 reverses the orientation of vectors, one can show that

$$\mathcal{K}_4(\varepsilon) = \frac{3 + 46\varepsilon + 52\varepsilon^2 + 8\varepsilon^3}{1 + 2\varepsilon - 4\varepsilon^2 - 8\varepsilon^3} - \frac{12\varepsilon + 14}{1 - 4\varepsilon^2} k_5(\varepsilon).$$

Let $L(\varepsilon)$ be the linear approximation for $k_5(\varepsilon)$,

$$\begin{aligned} L(\varepsilon) &= \frac{\varepsilon - \varepsilon_0}{\varepsilon_2 - \varepsilon_0} (k_5(\varepsilon_2) - k_5(\varepsilon_0)) + k_5(\varepsilon_0) \\ &= \frac{\varepsilon - \varepsilon_0}{\varepsilon_2 - \varepsilon_0} (k_5^- - k_5^+) + k_5^+. \end{aligned}$$

One can verify that $\frac{d}{d\varepsilon} k_5 < 0$ and $\frac{d^2}{d\varepsilon^2} k_5 > 0$ for $\varepsilon_0 < \varepsilon \leq \varepsilon_2$, so that $L(\varepsilon) > k_5(\varepsilon)$ across this parameter range and is equal at its extremes. This implies

$$\mathcal{K}_4(\varepsilon) \geq \frac{3 + 46\varepsilon + 52\varepsilon^2 + 8\varepsilon^3}{1 + 2\varepsilon - 4\varepsilon^2 - 8\varepsilon^3} - \frac{12\varepsilon + 14}{1 - 4\varepsilon^2} L(\varepsilon) := \mathcal{B}_2(\varepsilon)$$

To show condition (11), and complete this final case, it is sufficient to show that

$$\mathcal{B}_1(\varepsilon)\mathcal{B}_2(\varepsilon) > c \approx 1.4765. \tag{13}$$

One can show that $\mathcal{B}_1(\varepsilon)\mathcal{B}_2(\varepsilon)$ is monotone increasing (“Appendix”) over $\varepsilon_0 < \varepsilon \leq \varepsilon_2$ and therefore takes its minimal value at ε_0 . Plugging in this value gives

$$\mathcal{B}_1(\varepsilon_0)\mathcal{B}_2(\varepsilon_0) \approx 1.532235,$$

which establishes (13).

The case where $\text{diam}(\Gamma^1) = 0$ follows as a trivial consequence. $\mathcal{B}_1(\varepsilon)$ is still a lower bound for the proportion of Γ_{p-1} in $A_3 \cup A_4$, so we only need to compare $\mathcal{B}_1(\varepsilon)\mathcal{B}_2(\varepsilon)$ against $c = 1$ in this case. \square

One can follow an entirely analogous argument to prove the equivalent lemma for growth in forwards time:

Lemma 7 *Let Γ_{p-1} be a piecewise linear curve satisfying*

- (C0') Γ_{p-1} does not double back on itself,
- (C1') $\Gamma_{p-1} \subset \mathfrak{a}$,
- (C2') Each line segment in Γ_{p-1} is aligned with some vector in the minimal invariant cone \mathcal{C} for H ,

and which has simple intersection with each of the \mathfrak{a}_i . There exists a piecewise linear curve Γ_p satisfying (C0), (C1), (C2),

- (C3') $\Gamma_p \subset H^i(\Gamma_{p-1})$ for a chosen $i \in \{1, 2, 3\}$,
- (C4') There exists $\delta > 0$ such that $\text{diam}(\Gamma_p) \geq (1 + \delta) \text{diam}(\Gamma_{p-1})$,

where we measure the diameter of a curve using its projection to the y -axis.

We now give the argument for mapping into h -segments and v -segments, whose definitions we generalise to piecewise linear curves which connect the relevant boundaries of A_1 .

Lemma 8 *Let $\Gamma_P \subset A$ be a piecewise linear curve with each of its line segments aligned with a vector in C' . If Γ_P has non-simple intersection with some A_i , then $H^{-k}(\Gamma_P)$ contains a h -segment for some $k \in \{0, 4\}$.*

Proof In comparison with Lemma 5, we have fewer non-trivial cases to consider. We claim that any Γ_P which has non-simple intersection with A_2 contains a h -segment, that is, it can only connect A_2 to itself by traversing A_1 . Since if Γ_P were to connect the two parts of A_2 through A_3 , it would have to contain a segment with gradient

$$g < \frac{\frac{1}{2} - \varepsilon - 2\varepsilon}{\frac{1}{2} - \varepsilon - (\frac{1}{2} + \varepsilon)} = -\frac{1 - 6\varepsilon}{4\varepsilon} =: h(\varepsilon),$$

the gradient of the line segment joining the points $(\frac{1}{2} - \varepsilon, \frac{1}{2} - \varepsilon)$ and $(\frac{1}{2} + \varepsilon, 2\varepsilon)$. However, g is bounded from below by $g_3''(\varepsilon)$ with

$$g_3''(\varepsilon) \geq g_3''(\varepsilon_2) \approx -0.6688$$

across $\varepsilon_0 < \varepsilon \leq \varepsilon_2$. Now

$$h(\varepsilon) \leq h(\varepsilon_2) \approx -1.4397$$

across the range, so that $g > h(\varepsilon)$ at each ε . Hence, if Γ_P has non-simple intersection with A_2 , it follows that it contains a h -segment. The same clearly holds if Γ_P has non-simple intersection with A_3 .

Assume, then, that Γ_P has non-simple intersection with A_1 . This implies that Γ_P connects the two sloping boundaries of A_1 through $b = A_2 \cup A_3$. We will show that $H^{-4}(\Gamma_P)$ contains a h -segment. Figure 12 shows a region $\mathfrak{D} \subset b$, bounded by two piecewise linear curves ω, ζ . These curves can be defined by their end points on ∂b and their turning points, whose full coordinates will be given in as supplementary material. Label these points as $\omega_j, \zeta_j, j = 1, 2, 3, 4$ so that the x -coordinate increases with j . These curves (and hence \mathfrak{D}) are contained within b for $\varepsilon \leq \varepsilon_2$, with ζ_2 limiting onto the right boundary of b ($y = x - \frac{1}{2} + \varepsilon$) as $\varepsilon \rightarrow \varepsilon_2$. In particular, $\varepsilon_2 \approx 0.08504$ is the positive solution to the cubic equation

$$8\varepsilon^3 + 20\varepsilon^2 + 10\varepsilon - 1 = 0.$$

The argument for mapping into h -segments is roughly analogous to that given for the η -perturbation. Applying H^{-4} to \mathfrak{D} gives a quadrilateral in A_1 with sides on its left and right boundaries (the images of ζ and ω under H^{-4}). Clearly any Γ_P which joins the left and right sides of b must join ω and ζ through \mathfrak{D} . Let Γ be this part of the curve, then $H^{-4}(\Gamma)$ must be a piecewise linear curve joining $H^{-4}(\omega)$ and $H^{-4}(\zeta)$ through $H^{-4}(\mathfrak{D})$. That is, $H^{-4}(\Gamma)$ is a h -segment. \square

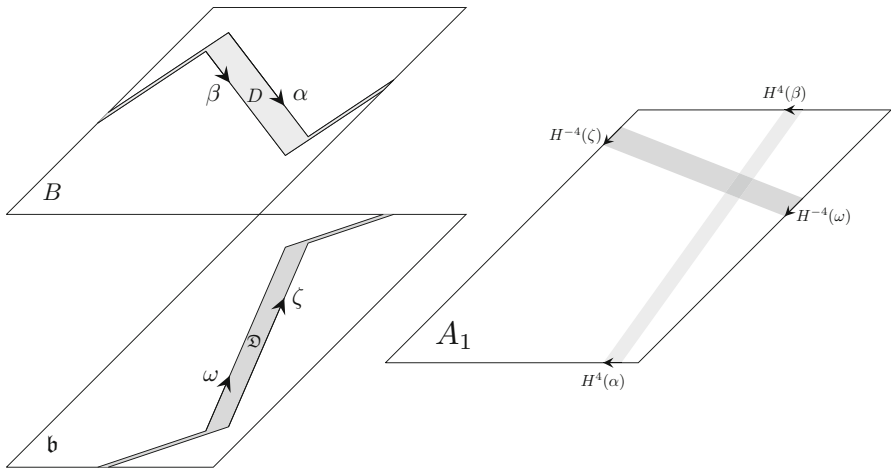


Fig. 12 Left: Two regions $\mathfrak{D} \subset \mathfrak{b}$ and $D \subset B$, bounded by the piecewise linear curves ω, ζ and α, β , respectively. Right: Their images in A_1 under H^{-4} and H^4 , respectively, establishing h - and v -segments

Lemma 9 *Let $\Gamma_P \subset \mathfrak{a}$ be a piecewise linear curve with each of its line segments aligned with a vector in \mathcal{C} . If Γ_P has non-simple intersection with some \mathfrak{a}_i , then $H^k(\Gamma_P)$ contains a v -segment for some $k \in \{0, 4\}$.*

Proof Analogous to the previous lemma, non-simple intersection with \mathfrak{a}_2 or \mathfrak{a}_3 imply that Γ_P already contains a v -segment. To see this, note that if Γ_P connected the two parts of \mathfrak{a}_2 through \mathfrak{a}_3 , it would have to contain a segment with gradient

$$g(\varepsilon) > \frac{\frac{1}{2} - \varepsilon}{2\varepsilon} =: h(\varepsilon).$$

However $g(\varepsilon)$ is bounded from above by the anti-clockwise invariant cone boundary $g_3^u(\varepsilon)$ and

$$g_3^u(\varepsilon) \leq g_3^u(\varepsilon_2) \approx 1.669 < 2.440 \approx h(\varepsilon_2) \leq h(\varepsilon)$$

across $\varepsilon_0 < \varepsilon \leq \varepsilon_2$. As before, then, it remains to assess the case where Γ_P has non-simple intersection with \mathfrak{a}_1 . It follows that Γ_P joins the upper and lower boundaries of B through B . Figure 12 shows a region D bounded by ∂B and two piecewise linear curves α, β . These curves are contained within B across $\varepsilon_0 < \varepsilon \leq \varepsilon_2$, with \mathfrak{a}_2 limiting onto the line $y = 1$ as $\varepsilon \rightarrow \varepsilon_2$. Applying H^4 to D gives a quadrilateral spanning across A_1 , with sides $H^4(\alpha), H^4(\beta)$ on its lower and upper boundaries, respectively. Clearly Γ_P must connect β to α through D , and therefore $H^4(\Gamma_P)$ contains a v -segment. \square

We are now ready to establish ergodicity over $\varepsilon_0 < \varepsilon < \varepsilon_2$.

Proof of Proposition 5 By the same argument given in the proof of Proposition 2, by Lemmas 1, 7, 9, given any $z \in X'$ we can find m such that $H^m(\gamma_u(z))$ contains a v -segment. Similarly by Lemmas 1, 6, 8, given any $z' \in X'$ we can find n such that

$H^{-n}(\gamma_s(z'))$ contains a h -segment. It follows that they intersect which, since z and z' were arbitrary, establishes (M). \square

5.3 Establishing the Bernoulli Property

Proposition 6 *Condition (MR) holds for H when $\varepsilon_0 < \varepsilon \leq \varepsilon_2$.*

Proof Follow the same argument given in the proof of Proposition 3, replacing η by $\frac{1}{2} - \varepsilon$. \square

We are now ready to prove the main theorem.

Proof of Theorem 1 Noting that (KS1) and (KS2) were trivially satisfied, the Bernoulli property holds for H over $0 < \eta < \eta_1$ by Theorem 2 and Propositions 1, 2, and 3. Let $\eta_2 = \frac{1}{2} - \varepsilon_2$ and $\eta_3 = \frac{1}{2} - \varepsilon_0$. Then, H is also Bernoulli over $\eta_2 \leq \eta < \eta_3$ by Theorem 2 and Propositions 4, 5, and 6. \square

6 Final Remarks

In summary, over the parameter range $0 < \eta < \frac{1}{2}$ we have given two windows within which we can prove global hyperbolicity and two subsets where mixing results can be established. A natural question is whether these are the largest sets in which these properties hold. For hyperbolicity, the bounds appear optimal, with island structures developing around period 3 orbits when $\frac{1}{3} < \eta < \frac{1}{2} - \varepsilon_1$. The itinerary for these orbits (and some neighbourhood around them) is $BCA BCA BCA \dots$ so stretching behaviour is determined by the matrix M_3 , which is non-hyperbolic. For the mixing property, the parameter limits given are not optimal. For example, ε_2 is not the highest upper bound on the ε -mixing window that our analysis allows for, but it is very close. By considering a 5-iterate mapping into h - and v -segments, this bound could be increased only very slightly. Improving the bound $B_1(\varepsilon)$ would increase it further, but would in turn complicate the already lengthy algebraic manipulations.

When following the Katok and Strelcyn approach, it is typical to be left with parameter ranges where non-uniform hyperbolicity can be established, but proving the mixing property is more challenging. See, for example, the families of maps studied in Przytycki (1983) and Wojtkowski (1981). In both of these examples, the strength of the shears is increased to break up elliptic islands and ensure an invariant cone. Indeed, the (Wojtkowski 1981; Bullett 1986) map at parameter value $K = 4$ exhibits similar dynamics to a variation of Cerbelli and Giona's map with a double strength non-monotonic shear, i.e. taking $H = G \circ F^2$. In contrast, for the perturbation considered in this work the shear strength is not varied, in particular $\int_0^1 f(y) dy$ is independent of η .

The cornerstone of our method was establishing a partition of returns and constructing an invariant expanding cone, both to prove nonzero Lyapunov exponents and as a basis for understanding how images of local manifolds grow in diameter. This approach seems viable for proving mixing properties in other systems. For example, consider the variation of Cerbelli and Giona's map, perturbing the second shear by

$G(x, y) = (x, y + (1 + \delta)x) \bmod 1$. Nonzero Lyapunov exponents can be established by our method for $0 < \delta < \delta_1 \approx 0.281$, but proving **(M)** is more challenging, largely due to the map's discontinuity cutting up the images of local manifolds.

Towards the goal of more closely resembling realistic fluid velocity profiles, natural extensions to this work include introducing non-monotonicity to the second shear and studying smooth perturbations. Both of these increase the number of derivative matrices acting on the system, which complicates the analysis. The first of these is addressed in Myers Hill et al. (2021), taking G similar to F in the present article. The second is considerably more challenging and is the subject of ongoing work.

Supplementary Information The online version contains supplementary material available at <https://doi.org/10.1007/s00332-022-09790-0>.

Acknowledgements JMH is supported by EPSRC under Grant Ref. EP/L01615X/1.

Data Availability Statement Data sharing is not applicable to this article as no datasets were generated or analysed during the current study.

Open Access This article is licensed under a Creative Commons Attribution 4.0 International License, which permits use, sharing, adaptation, distribution and reproduction in any medium or format, as long as you give appropriate credit to the original author(s) and the source, provide a link to the Creative Commons licence, and indicate if changes were made. The images or other third party material in this article are included in the article's Creative Commons licence, unless indicated otherwise in a credit line to the material. If material is not included in the article's Creative Commons licence and your intended use is not permitted by statutory regulation or exceeds the permitted use, you will need to obtain permission directly from the copyright holder. To view a copy of this licence, visit <http://creativecommons.org/licenses/by/4.0/>.

7 Appendix

7.1 Establishing the Lower Bound $\mathcal{B}_1(\varepsilon)$

In this section, we derive a lower bound

$$\frac{\text{diam}(\Gamma^4)}{\text{diam}(\Gamma^4) + \text{diam}(\Gamma^5)} > \mathcal{B}_1(\varepsilon)$$

on the proportions of a piecewise linear curve Γ_{p-1} , constrained by the invariant cone, in the regions A_4 and A_5 . We do this by maximising $\text{diam}(\Gamma^5)$ and minimising $\text{diam}(\Gamma^4)$, i.e. we assume that Γ_{p-1} takes the longest possible path (in diameter) across A_5 , and the shortest possible path across A_4 . These are straight line segments, each aligned with one of the cone boundaries. Write the gradient of segments across A_4 and A_5 as k_4 and k_5 , respectively. We now have to choose where on the L_1 (boundary between A_4 and A_5) Γ_{p-1} intersects so that the proportion in A_4 is minimal. The lines where each segment terminates are shown in Fig. 13a. Note that L_2 is the line $y = k_2x$, and L_3 is the line $y = x - (\frac{1}{2} - \varepsilon)$. The diameter of the A_4 segment passing

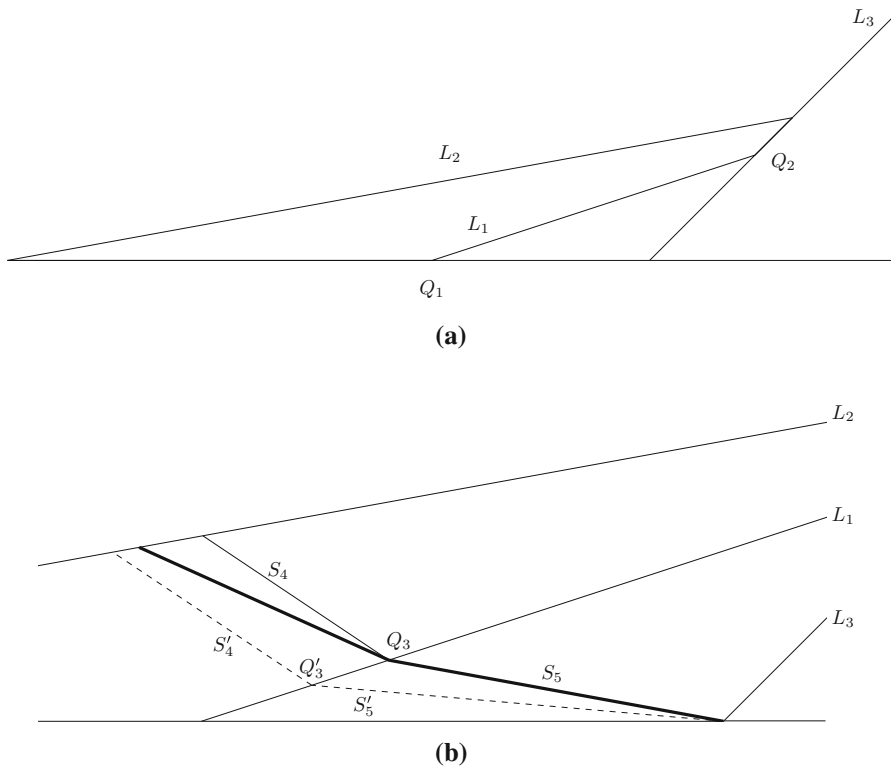


Fig. 13 A close-up on the lower portion of A_2 , $\varepsilon = 0.05$. Part **a** shows the lines which bound the regions A_4 and A_5 . Part **b** shows the curve (thickest line) across A_2 which minimises (12), crossing L_1 at Q_3 . Also shown is the segments S_4 which provides a lower bound for its diameter in A_4 . Segments S'_4 and S'_5 are defined to give further bound on (12) with minimal ε dependence

through $(x_1, y_1) \in L_1$ is given by

$$\text{diam}(\Gamma^4) = x_1 - \frac{y_1 - k_4x_1}{k_2 - k_4} \tag{14}$$

and the diameter of the A_5 segment passing through $(x_1, y_1) \in L_1$ is given by

$$\text{diam}(\Gamma^5) = \frac{y_1 + (\frac{1}{2} - \varepsilon) - k_5x_1}{1 - k_5} - x_1, \tag{15}$$

valid for $(x_1, y_1) \in L_1$ above a certain threshold. This is the point Q_3 , defined as the intersection of L_1 with the line $y = k_5(x - \frac{1}{2} + \varepsilon)$, the lowest point on L_1 such that the segment in A_5 still intersects $L_3 \cap A$. We claim that Q_3 is the point where the proportion (12) is minimal. To see this, note that as we move along the L_1 from Q_2 to Q_3 , both diameters grow linearly. Parameterise the path as $Q_2(1 - z) + Q_3z$ for $z \in [0, 1]$. Now, at each ε , $\text{diam}(\Gamma^4)(z)$ grows like $m_4z + c_4$ for some $m_4 > 0$, and $c_4 > 0$ the diameter of the segment in A_4 passing through Q_2 . Next, $\text{diam}(\Gamma^5)(z)$

grows like m_5z for some $m_5 > 0$ since it grows from 0. Now

$$\begin{aligned} \frac{\text{diam}(\Gamma^4)}{\text{diam}(\Gamma^4) + \text{diam}(\Gamma^5)}(z) &= 1 - \frac{\text{diam}(\Gamma^5)}{\text{diam}(\Gamma^4) + \text{diam}(\Gamma^5)}(z) \\ &= 1 - \frac{m_5z}{m_4z + c_4 + m_5z} \\ &= 1 - \frac{1}{\frac{c_4}{m_5z} + \frac{m_4}{m_5} + 1} \end{aligned}$$

which is minimal at $z = 1$, so (12) is minimal at Q_3 . We will now derive a lower bound on (12) which has weaker ε dependence.

Figure 13b shows the path through Q_3 in bold. Its gradient in A_5 is given by $k_5(\varepsilon)$, aligned with the unstable eigenvector of \mathfrak{M}_2 . Its gradient in A_4 is given by $k_4(\varepsilon)$, aligned with the unstable eigenvector of \mathfrak{M}_3 . Writing the segment in A_5 as S_5 , note that

$$\frac{\text{diam}(\Gamma^4)}{\text{diam}(\Gamma^4) + \text{diam}(\Gamma^5)} \geq \frac{\text{diam}(S_4)}{\text{diam}(S_4) + \text{diam}(S_5)}$$

where S_4 is the segment in A_4 connecting Q_3 with L_2 , with gradient aligned with the steepest possible $k_4(\varepsilon)$ over the parameter range, $k_4^- = \inf_{\varepsilon} k_4(\varepsilon) \approx -0.6688$.⁶ We have equality at $\varepsilon = \varepsilon_2$.

Now define S'_5 as we did S_5 , but aligned with the least steep gradient in the parameter range, $k_5^+ = \sup_{\varepsilon} k_5(\varepsilon) = k_5(\varepsilon_0) \approx -0.08750$. Write its point of intersection with L_1 as Q'_3 . Note that $Q_3 = Q'_3$ when $\varepsilon = \varepsilon_0$. Define S'_4 as having the same gradient as S_4 , but passing through Q'_3 .

We claim that

$$\frac{\text{diam}(S_4)}{\text{diam}(S_4) + \text{diam}(S_5)} \geq \frac{\text{diam}(S'_4)}{\text{diam}(S'_4) + \text{diam}(S'_5)} \tag{16}$$

with equality at $\varepsilon = \varepsilon_0$. Barring this case, note that the inequality is not immediate as both $\text{diam}(S'_4) > \text{diam}(S_4)$ and $\text{diam}(S'_5) > \text{diam}(S_5)$. Assume the non-trivial case $\varepsilon > \varepsilon_0$ and rewrite (16) as

$$\frac{1}{1 + \frac{\text{diam}(S_5)}{\text{diam}(S_4)}} > \frac{1}{1 + \frac{\text{diam}(S'_5)}{\text{diam}(S'_4)}}$$

which is equivalent to

$$\frac{\text{diam}(S_5)}{\text{diam}(S_4)} < \frac{\text{diam}(S'_5)}{\text{diam}(S'_4)}. \tag{17}$$

⁶ The minus sign in k_4^- refers to it being the clockwise bound on the invariant cone.

Define the diameter differences $\Delta_i = \text{diam}(S'_i) - \text{diam}(S_i)$ and write Q_3 as (x_1, y_1) , Q'_3 as (x'_1, y'_1) , and Q_1 as $(x_0, 0)$. Then $\Delta_5 = x_1 - x'_1$. We can solve the line intersection equations to show that

$$\begin{aligned} \text{diam}(S_4) &= x_1 - \frac{y_1 - k_4^- x_1}{k_2 - k_4} \\ &= \frac{k_2 x_1 - y_1}{k_2 - k_4^-} \end{aligned} \tag{18}$$

so that

$$\begin{aligned} \Delta_4 &= x_1 - \frac{k_2 x'_1 - y'_1 - k_2 x_1 + y_1}{k_2 - k_4^-} \\ &= \frac{k_2(x'_1 - x_1) + k_1(x_1 - x'_1)}{k_2 - k_4^-} \\ &= \frac{k_1 - k_2}{k_2 - k_4^-} \Delta_5. \end{aligned} \tag{19}$$

We can rewrite (17) as

$$\frac{\text{diam}(S'_5) - \Delta_5}{\text{diam}(S'_4) - \Delta_4} < \frac{\text{diam}(S'_5)}{\text{diam}(S'_4)},$$

which rearranges to

$$\frac{\Delta_4}{\Delta_5} < \frac{\text{diam}(S'_4)}{\text{diam}(S'_5)}.$$

By (19), (18), and $y'_1 = k_1(x'_1 - x_0)$ this is

$$\frac{k_1 - k_2}{k_2 - k_4^-} < \frac{\frac{k_2 x'_1 - k_1(x'_1 - x_0)}{k_2 - k_4^-}}{\frac{1}{2} - \varepsilon - x'_1},$$

which can be simplified to $(k_1 - k_2) (\frac{1}{2} - \varepsilon) < k_1 x_0$. So (17) holds, provided that

$$\frac{12\varepsilon^2 + 16\varepsilon + 1}{(2\varepsilon + 1)(2\varepsilon + 5)} - \frac{4\varepsilon}{2\varepsilon + 1} < \frac{12\varepsilon^2 + 16\varepsilon + 1}{(2\varepsilon + 1)(2\varepsilon + 5)} \cdot \frac{-4\varepsilon^3 - 2\varepsilon^2 + \varepsilon + \frac{1}{2}}{12\varepsilon^2 + 16\varepsilon + 1},$$

which reduces to $1 - 4\varepsilon + 4\varepsilon^2 < (1 + 2\varepsilon)^2$, valid for all $\varepsilon > 0$. This verifies the claim, giving us a lower bound

$$\frac{\text{diam}(\Gamma^4)}{\text{diam}(\Gamma^4) + \text{diam}(\Gamma^5)} \geq \frac{\text{diam}(S'_4)}{\text{diam}(S'_4) + \text{diam}(S'_5)} = \frac{k_2 x'_1 - y'_1}{(\frac{1}{2} - \varepsilon)(k_2 - k_4^-) - y'_1 + k_4^- x'_1}.$$

Noting that y'_1 is very small and positive,⁷ removing it from the denominator gives a new bound

$$\frac{\text{diam}(\Gamma^4)}{\text{diam}(\Gamma^4) + \text{diam}(\Gamma^5)} > \frac{k_2x'_1 - y'_1}{\left(\frac{1}{2} - \varepsilon\right)(k_2 - k_4^-) + k_4^-x'_1} := \mathcal{B}_1(\varepsilon)$$

which has fewer terms to consider and is still a sufficiently strong bound for our purposes.

7.2 Expanding the Expression for $\mathcal{B}_1(\varepsilon)$

We will now show the expanded form of $\mathcal{B}_1(\varepsilon)$,

$$\begin{aligned} & \frac{k_2x'_1 - y'_1}{\left(\frac{1}{2} - \varepsilon\right)(k_2 - k_4^-) + k_4^-x'_1} \\ &= \frac{(2\varepsilon + 1)(2\varepsilon + 1 - 2k_5^+)}{(2\varepsilon + 1)(-k_4^-(2\varepsilon + 3) - k_5^+(2\varepsilon + 5)) + 12\varepsilon^2 + 16\varepsilon + 1}. \end{aligned} \tag{20}$$

To simplify the notation, let $x = x'_1$, $k_4 = k_4^-$ and $k_5 = k_5^+$. Then, $y'_1 = k_1(x - x_0)$ and we can write

$$\mathcal{B}_1(\varepsilon) = \frac{(k_2 - k_1)x + k_1x_0}{k_4x + \left(\frac{1}{2} - \varepsilon\right)(k_2 - k_4)} \tag{21}$$

Let $\varphi = 2(1 + 2\varepsilon)(5 + 2\varepsilon)$. Then $\varphi k_1 = 24\varepsilon^2 + 32\varepsilon + 2$, $\varphi k_1x_0 = -8\varepsilon^3 - 4\varepsilon^2 + 2\varepsilon + 1$, and $\varepsilon k_2 = 8\varepsilon(2\varepsilon + 5)$ so that multiplying (21) by φ/φ yields

$$\begin{aligned} \mathcal{B}_1(\varepsilon) &= \frac{(8\varepsilon(2\varepsilon + 5) - (24\varepsilon^2 + 32\varepsilon + 2))x - 8\varepsilon^3 - 4\varepsilon^2 + 2\varepsilon + 1}{k_4\varphi x + \left(\frac{1}{2} - \varepsilon\right)(8\varepsilon(2\varepsilon + 5) - k_4\varphi)} \\ &= \frac{(-8\varepsilon^2 + 8\varepsilon - 2)x + (1 - 2\varepsilon)(2\varepsilon + 1)^2}{k_4\varphi x + (1 - 2\varepsilon)(2\varepsilon + 5)(4\varepsilon - k_4(2\varepsilon + 1))} \\ &= \frac{-2(1 - 2\varepsilon)^2x + (1 - 2\varepsilon)(2\varepsilon + 1)^2}{k_4\varphi x + (1 - 2\varepsilon)(2\varepsilon + 5)(4\varepsilon - k_4(2\varepsilon + 1))} \\ &= \frac{-2(1 - 2\varepsilon)x + (2\varepsilon + 1)^2}{\frac{k_4\varphi x}{1 - 2\varepsilon} + (2\varepsilon + 5)(4\varepsilon - k_4(2\varepsilon + 1))}. \end{aligned}$$

Now by

$$\begin{aligned} x &= \frac{k_5(\varepsilon - \frac{1}{2}) + k_1x_0}{k_1 - k_5} \\ &= \frac{-k_5(2\varepsilon + 5)(1 - 2\varepsilon) + (1 - 2\varepsilon)(1 + 2\varepsilon)}{2(2\varepsilon + 5)(k_1 - k_5)}, \end{aligned}$$

⁷ Also noting that the numerator and denominator are both positive.

we have that

$$\frac{k_4 \varphi x}{1 - 2\varepsilon} = k_4(2\varepsilon + 1) \frac{-k_5(2\varepsilon + 5) + 1 + 2\varepsilon}{k_1 - k_5} \tag{22}$$

and

$$-2(1 - 2\varepsilon)x = \frac{k_5(1 - 2\varepsilon)^2}{k_1 - k_5} - \frac{(1 - 2\varepsilon)^2(1 + 2\varepsilon)}{(2\varepsilon + 5)(k_1 - k_5)} \tag{23}$$

so that

$$\begin{aligned} \mathcal{B}_1(\varepsilon) &= \frac{k_5(2\varepsilon - 1)^2(2\varepsilon + 5) - (1 - 2\varepsilon)^2(1 + 2\varepsilon) + (2\varepsilon + 1)^2(2\varepsilon + 5)(k_1 - k_5)}{k_4(2\varepsilon + 1)(2\varepsilon + 5)(-k_5(2\varepsilon + 5) + 1 + 2\varepsilon) + (2\varepsilon + 5)^2(k_1 - k_5)(4\varepsilon - k_4(2\varepsilon + 1))}, \end{aligned}$$

where we have substituted in (22), (23) and multiplied top and bottom by $(2\varepsilon + 5)(k_1 - k_5)$. Write its numerator and denominator as $N(\varepsilon)$ and $D(\varepsilon)$. Expanding the k_1 term,

$$\begin{aligned} N(\varepsilon) &= k_5(2\varepsilon + 5) \left((2\varepsilon - 1)^2 - (2\varepsilon + 1)^2 \right) + (2\varepsilon + 1)(12\varepsilon^2 + 16\varepsilon + 1 - (1 - 2\varepsilon)^2) \\ &= -8\varepsilon k_5(2\varepsilon + 5) + (2\varepsilon + 1)(8\varepsilon^2 + 20\varepsilon) \\ &= (2\varepsilon + 5)(4\varepsilon(2\varepsilon + 1) - 8\varepsilon k_5(2\varepsilon + 5)) \end{aligned}$$

and

$$\begin{aligned} D(\varepsilon) &= k_4(2\varepsilon + 1)(2\varepsilon + 5) (-k_5(2\varepsilon + 5) + 1 + 2\varepsilon) - k_5(2\varepsilon + 5)^2(4\varepsilon - k_4(2\varepsilon + 1)) \\ &\quad + \frac{12\varepsilon^2 + 16\varepsilon + 1}{2\varepsilon + 1} (2\varepsilon + 5) (4\varepsilon - k_4(2\varepsilon + 1)) \\ &= (2\varepsilon + 5) \left(k_4 \left[(2\varepsilon + 1)(-k_5(2\varepsilon + 5) + 1 + 2\varepsilon) + k_5(2\varepsilon + 5)(2\varepsilon + 1) \right. \right. \\ &\quad \left. \left. - (12\varepsilon^2 + 16\varepsilon + 1) \right] \right. \\ &\quad \left. - 4\varepsilon k_5(2\varepsilon + 5) + \frac{4\varepsilon}{2\varepsilon + 1} (12\varepsilon + 16\varepsilon + 1) \right). \end{aligned}$$

Noting that the $k_4 k_5$ terms cancel and $(1 + 2\varepsilon)^2 - (12\varepsilon^2 + 16\varepsilon + 1) = -4\varepsilon(2\varepsilon + 3)$,

$$\mathcal{B}_1(\varepsilon) = \frac{4\varepsilon(2\varepsilon + 1) - 8\varepsilon k_5}{-4\varepsilon k_4(2\varepsilon + 3) - 4\varepsilon k_5(2\varepsilon + 5) + \frac{4\varepsilon}{2\varepsilon + 1}(12\varepsilon^2 + 16\varepsilon + 1)}.$$

Multiplying top and bottom by $\frac{2\varepsilon + 1}{4\varepsilon}$ establishes (20).

7.3 $\mathcal{B}_1(\varepsilon)\mathcal{B}_2(\varepsilon)$ is Monotone Increasing

Starting with the bound on $K_4(\varepsilon)$,

$$\begin{aligned} \mathcal{B}_2(\varepsilon) &= \frac{3 + 46\varepsilon + 52\varepsilon^2 + 8\varepsilon^3}{1 + 2\varepsilon - 4\varepsilon^2 - 8\varepsilon^3} - \frac{12\varepsilon + 14}{1 - 4\varepsilon^2}L(\varepsilon) \\ &= \frac{3 + 46\varepsilon + 52\varepsilon^2 + 8\varepsilon^3}{(1 - 2\varepsilon)(1 + 2\varepsilon)^2} - \frac{12\varepsilon + 14}{(1 - 2\varepsilon)(1 + 2\varepsilon)}L(\varepsilon) \\ &= \frac{3 + 46\varepsilon + 52\varepsilon^2 + 8\varepsilon^3 - (1 + 2\varepsilon)(12\varepsilon + 14)L(\varepsilon)}{(1 - 2\varepsilon)(1 + 2\varepsilon)^2}. \end{aligned}$$

Combining with our expanded expression for $\mathcal{B}_1(\varepsilon)$,

$$\begin{aligned} \mathcal{B}_1(\varepsilon)\mathcal{B}_2(\varepsilon) &= \frac{(2\varepsilon + 1 - 2k_5^+)(3 + 46\varepsilon + 52\varepsilon^2 + 8\varepsilon^3 - (1 + 2\varepsilon)(12\varepsilon + 14)L(\varepsilon))}{(1 - 2\varepsilon)(1 + 2\varepsilon)^2(-k_4^-(2\varepsilon + 3) - k_5^+(2\varepsilon + 5)) + (1 - 2\varepsilon)(1 + 2\varepsilon)(12\varepsilon^2 + 16\varepsilon + 1)} \end{aligned}$$

where we have divided through by $(1 + 2\varepsilon)/(1 + 2\varepsilon)$. Write its numerator and denominator as $P(\varepsilon)$ and $Q(\varepsilon)$, then $\mathcal{B}_1(\varepsilon)\mathcal{B}_2(\varepsilon)$ is monotone increasing if $P'Q - PQ' > 0$. Note that as a linear function, $L'(\varepsilon) = k_6 \approx -1.85175$ is constant. The factors derived from P are then

$$\begin{aligned} P(\varepsilon) &= (2\varepsilon + 1 - 2k_5^+)(3 + 46\varepsilon + 52\varepsilon^2 + 8\varepsilon^3 - (24\varepsilon^2 + 40\varepsilon + 14)L(\varepsilon)), \\ P'(\varepsilon) &= 6 + 92\varepsilon + 104\varepsilon^2 + 16\varepsilon^3 - (48\varepsilon^2 + 80\varepsilon + 28)L(\varepsilon) \\ &\quad + (2\varepsilon + 1 - 2k_5^+)(46 + 104\varepsilon + 24\varepsilon^2 - (48\varepsilon + 40)L(\varepsilon) \\ &\quad - k_6(24\varepsilon^2 + 40\varepsilon + 14)) \end{aligned}$$

which, since $(2\varepsilon + 1 - 2k_5^+) > 0$, $L(\varepsilon) < 0$, and $k_6 < 0$, are both positive for $\varepsilon > 0$. Hence, over the parameter range $\varepsilon_0 < \varepsilon \leq \varepsilon_2$, P is maximal at ε_2 . Differentiating again, one can verify that $P'' > 0$, so that P' is bounded below by $P'(\varepsilon_0)$. Now for the factors derived from the denominator,

$$\begin{aligned} Q(\varepsilon) &= (8\varepsilon^3 + 4\varepsilon^2 - 2\varepsilon_1)(k_4^-(2\varepsilon + 3) + k_5^+(2\varepsilon + 5)) + (1 - 4\varepsilon^2)(12\varepsilon^2 + 16\varepsilon + 1), \\ Q'(\varepsilon) &= (24\varepsilon^2 + 8\varepsilon - 2)(k_4^-(2\varepsilon + 3) + k_5^+(2\varepsilon + 5)) \\ &\quad + (8\varepsilon^3 + 4\varepsilon^2 - 2\varepsilon_1)(2k_4^- + 2k_5^+) \\ &\quad - 8\varepsilon(12\varepsilon^2 + 16\varepsilon + 1) + (1 - 4\varepsilon^2)(24\varepsilon + 16) \end{aligned}$$

which, since $8\varepsilon^3 + 4\varepsilon^2 - 2\varepsilon_1 < 0$ and $-8\varepsilon(12\varepsilon^2 + 16\varepsilon + 1) + (1 - 4\varepsilon^2)(24\varepsilon + 16) = 16 + 16\varepsilon + \dots > 0$ over the parameter range, are also both positive. Hence Q bounded below by $Q(\varepsilon_0)$. Again, one can verify that $Q'' < 0$ so that Q' is bounded above by $Q'(\varepsilon_0)$.

Hence, $P'Q - PQ' > P'(\varepsilon_0)Q(\varepsilon_0) - P(\varepsilon_2)Q'(\varepsilon_0) \approx 29.853$, positive as required.

References

- Bullett, S.: Invariant circles for the piecewise linear standard map. *Commun. Math. Phys.* **107.2**, 241–262 (1986)
- Cerbelli, S., Giona, M.: A continuous archetype of nonuniform chaos in area-preserving dynamical systems. *J. Nonlinear Sci.* **15.6**, 387–421 (2005)
- Cerbelli, S., Giona, M.: Characterization of nonuniform chaos in area-preserving nonlinear maps through a continuous archetype". *Chaos Solit. Fract.* **35.1**, 13–37 (2008)
- Childress, S., Gilbert, A.D.: *Stretch, Twist, Fold: The Fast Dynamo*, vol. 37. Springer Science & Business Media (1995)
- Chirikov, B.V.: Research concerning the theory of non-linear resonance and stochasticity. Tech. rep. CM-P00100691 (1971)
- Demers, M.F., Wojtkowski, M.P.: A family of pseudo-Anosov maps. *Nonlinearity* **22.7**, 1743–1760 (2009)
- Katok, A.: Bernoulli diffeomorphisms on surfaces. *Ann. Math.* **110.3**, 529–547 (1979)
- Keating, J.P.: The cat maps: quantum mechanics and classical motion. *Nonlinearity* **4.2**, 309 (1991)
- Katok, A., Strelcyn, J.-M.: *Invariant Manifolds, Entropy and Billiards. Smooth Maps with Singularities. Lecture Notes in Mathematics.* Springer-Verlag, Berlin Heidelberg (1986)
- Liverani, C.: Birth of an elliptic island in a chaotic sea. *Math. Phys. Electron. J.* **10**, 13 (2004) (Paper No. 1)
- Liverani, C., Wojtkowski, M.P.: Ergodicity in Hamiltonian systems. In: *Dynamics Reported*, pp. 130–202. Springer (1995)
- MacKay, R.S.: Cerbelli and Giona's Map Is Pseudo-Anosov and Nine Consequences. *J. Nonlinear Sci.* **16.4**, 415–434 (2006)
- Myers Hill, J., Sturman, R., Wilson, M.C.T.: Exponential mixing by orthogonal non monotonic shears. *Phys. D: Nonlinear Phenom.* **434**, 33224 (2022). <https://doi.org/10.1016/j.physd.2022.133224>
- Oseledets, V. I.: A multiplicative ergodic theorem. Lyapunov characteristic numbers for dynamical systems. *Trans. Moscow Math. Soc.* **19**, 197–231 (1968)
- Ott, E.: *Chaos in Dynamical Systems.* Cambridge university press (2002)
- Ottino, J.M.: *The kinematics of mixing: stretching, chaos, and transport*, vol. 3. Cambridge university press (1989)
- Pesin, Y.B.: Characteristic Lyapunov exponents and smooth ergodic theory. *Russian Math. Surv.* **32.4**, 55 (1977)
- Przytycki, F.: Ergodicity of toral linked twist mappings. *Annales scientifiques de l'École Normale Supérieure* **16.3**, 345–354 (1983)
- Pesin, Y., Senti, S., Zhang, K.: Thermodynamics of the Katok map. *Ergodic Theory Dyn. Syst.* **39.3**, 764–794 (2019)
- Sturman, R., Ottino, J.M., Wiggins, S.: *The Mathematical Foundations of Mixing: The Linked Twist Map as a Paradigm in Applications: Micro to Macro.* Cambridge University Press, Fluids to Solids. Cambridge Monographs on Applied and Computational Mathematics (2006)
- Sturman, R., Springham, J.: Rate of chaotic mixing and boundary behavior. *Phys. Rev. E* **87.1**, 012906 (2013)
- Springham, J., Sturman, R.: Polynomial decay of correlations in linked-twist maps. *Ergodic Theory Dyn. Syst.* **34.5**, 1724–1746 (2014)
- Vaienti, S.: Ergodic properties of the discontinuous sawtooth map. *J. Stat. Phys.* **67.1**, 251–269 (1992)
- Viana, M.: *Lectures on Lyapunov Exponents.* Cambridge Studies in Advanced Mathematics. Cambridge University Press, Cambridge (2014)
- Wojtkowski, M.: A model problem with the coexistence of stochastic and integrable behaviour. *Commun. Math. Phys.* **80.4**, 453–464 (1981)